Fault-Tolerant Synchronization of Drive-Response Memristive Competitive Neural Networks with Multiple Actuator Failures

Wenjing Duan, Yanli Huang, Quang Dan Le, Tse Chiu Wong

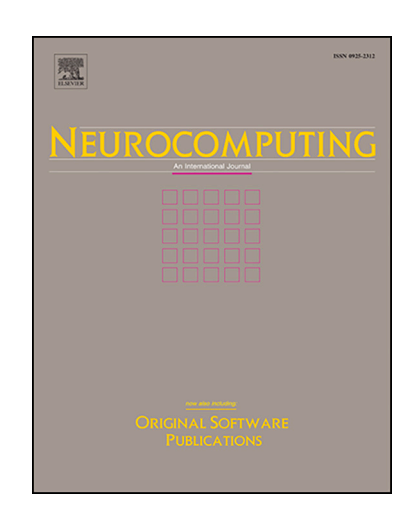
PII: S0925-2312(25)02161-7 DOI: https://doi.org/10.1016/j.

neucom.2025.131489

Reference: NEUCOM 131489

To appear in: Neurocomputing

Received Date: 15 June 2025
Revised Date: 30 July 2025
Accepted Date: 6 September 2025



Please cite this article as: Duan W, Huang Y, Le QD, Wong TC, Fault-Tolerant Synchronization of Drive-Response Memristive Competitive Neural Networks with Multiple Actuator Failures, *Neurocomputing* (2025), doi: https://doi.org/10.1016/j.neucom.2025.131489.

This is a PDF file of an unedited manuscript that has been accepted for publication. As a service to our customers we are providing this early version of the manuscript. The manuscript will undergo copyediting, typesetting, and review of the resulting proof before it is published in its final form. Please note that during the production process errors may be discovered which could affect the content, and all legal disclaimers that apply to the journal pertain.

© 2025 Elsevier B.V. All rights are reserved, including those for text and data mining, Al training, and similar technologies.

# Fault-Tolerant Synchronization of Drive-Response Memristive Competitive Neural Networks with Multiple Actuator Failures

Wenjing Duan<sup>a</sup>, Yanli Huang<sup>a,\*</sup>, Quang Dan Le<sup>b</sup>, Tse Chiu Wong<sup>c</sup>

<sup>a</sup> Tianjin Key Laboratory of Autonomous Intelligence Technology and Systems, School of Computer Science and Technology, Tiangong University, Tianjin 300387, China
 <sup>b</sup> College of Science and Engineering, University of Derby, Derby DE22 3AW, UK
 <sup>c</sup> Department of Design Manufacturing and Engineering Management, University of Strathclyde, Glasgow G1 1XJ, UK

#### Abstract

In this article, the synchronization of drive-response memristive competitive neural networks (MCNNs) under multiple actuator failures is studied through implementing fault-tolerant control scheme. Unlike previous studies, the actuator failures considered in this paper include both bias and effectiveness failures. To address these challenges, a proper mathematical model is firstly established to capture the impact of actuator failures on control inputs. Subsequently, several sufficient conditions are deduced by designing an appropriate bilayer fault-tolerant controller and constructing a Lyapunov functional to achieve the global exponential synchronization, finite-time synchronization, fixed-time synchronization and predefined-time synchronization respectively. Additionally, the settling time upper bounds for the proposed synchronization methods are determined. In the end, nu-

Email address: huangyanli@tiangong.edu.cn (Yanli Huang)

<sup>\*</sup>Corresponding author.

merical simulations with analysis and comparison are performed to confirm the validity of the proposed results.

Keywords: Fault-tolerant synchronization, multiple actuator failures, drive-response systems, memristive competitive neural networks

#### 1. Introduction

Synchronization represents a prevalent and extremely important dynamic behavior, which means that two or more subsystems exhibit consistent dynamic behavior. This behavior can be caused by the coupling between systems or external forces. It serves as the theoretical basis for understanding unknown dynamic systems with the help of one or more known dynamic systems and has made remarkable progress in numerous fields [1–4]. Based on the exponential stability theory, global exponential synchronization strategies have been proposed, which allows for a more effective way to utilize the known systems to understand the unknown ones [5–7]. The authors in [6] investigated the global exponential synchronization of discrete-time high-order bidirectional associative memory neural networks subject to multiple time-varying delays.

It is well-known that the synchronization process in most of existing results is typically analyzed in infinite-time. However, the driving-response system often requires rapid synchronization in practical applications to ensure real-time performance and reliability. Thus, Kamenkov [8] introduced the concept of finite-time stability initially in 1953. In finite-time synchronization [9–12], the settling time hinges on the initial state. But it is rather difficult to precisely determine the initial value of a system. Consequently,

the concept of fixed-time stability [13–16] was introduced to overcome this limitation. Liu et al. [14] investigated the robust fixed-time synchronization of fuzzy shunting-inhibitory cellular neural networks with time delays through the development of two distinct control strategies. Actually, fixedtime synchronization offers a precise upper bound for the settling time, and this bound is not determined by the initial state. However, this bound is not arbitrary, which renders that it is difficult to be adjusted according to the parameters of the system and controller. Consequently, the predefined-time synchronization theory was presented to address the challenge of settling time by providing an arbitrary bound that doesn't rely on initial conditions and can be set as a controller parameter. This allows for the network to be easily tuned in advance. In secure communication, it is essential that synchronization occurs within a predetermined time to meet the designer's requirements. In [17], the authors proposed a novel approach for Lyapunov-like characterizations that ensure predefined-time stability, integrating previous methods to create a unified framework for constructing dynamic systems with predefined-time stability and a sliding mode controller with predefined-time performance.

Over the past several decades, neural networks (NNs) have emerged as the focus of extensive research owing to their broad applications across fields such as computer science, signal processing, visual analytics, and so on [18– 20]. It is a common understanding that a key feature of dynamic NNs is the presence of both feedforward and feedback connections between neural layers. Additionally, it is recognized that synaptic weights in biological networks change over time. These aspects of dynamic NNs and the chang-

ing synaptic weights in biological networks set the stage for exploring more complex neural mechanisms. To further unravel this complexity, Cohen and Grossberg [21] introduced competitive NNs (CNNs) model for the first time in 1983, which integrates both activity and weight dynamics. These networks can store target patterns as stable equilibrium points, a property that relies on stability criteria to explain the complex interplay between neural activity and learning dynamics. Furthermore, CNNs not only describe the slow, unsupervised synaptic adjustments associated with long-term memory (LTM) but also represent the rapid neural activities linked to short-term memory (STM). CNNs have led to numerous significant research advancements due to the above-mentioned advantages [22–25]. In [24], the authors investigated the multistability properties of a class of CNNs with sigmoidal activation functions, incorporating state-dependent switching and fractional-order derivatives.

In 2008, HP team [26] fabricated a memristor device having memory properties. Memristors [27–30] can be better connected to large circuits in NNs compared to regular resistors, thus the calculating capacity, parallel working ability and self-adjusting abilities of NNs are significantly improved. Accordingly, memristors have been increasingly introduced into CNNs by academics to form memristive CNNs (MCNNs) [31–34]. Xu et al. [31] carried out an in-depth study on the fixed-time synchronization of complex-valued MCNNs affected by mixed delays. Gong et al. [34] carried out research on the synchronization issue of MCNNs with time-varying delay.

Although significant progress has been made in the synchronization of MCNNs, the matter of fault tolerance on this kind of network has failed

to garner adequate attention. Within practical applications, system failures are often unavoidable due to factors such as network disturbances and electromagnetic interference, which can severely impact network stability. Therefore, the study of fault-tolerant strategies for network synchronization is essential [35–42]. In [39], the global exponential synchronization of complex networks, incorporating node delay and a switching topology, was analyzed under an almost sure condition. In [40], the authors explored the synchronization issue relying on an observer for a class of complex dynamical networks in the presence of randomly occurring actuator defects, external disruptions, input saturation and time delay. However, most existing studies on fault-tolerant synchronization mainly focus on actuator effectiveness failures [41, 42], assuming that actuators either degrade partially or completely lose their function. In practical systems, actuators may also suffer from bias failures, where they produce constant erroneous outputs regardless of control signals. These two types of failures can occur independently or simultaneously, and ignoring either may lead to inaccurate modeling and reduced control reliability. To the best of our knowledge, few studies have addressed both bias and effectiveness failures in a unified framework, especially for drive-response MCNNs. This gap motivates us to design a fault-tolerant synchronization scheme that takes both failure types into account for better robustness and practical relevance.

Taking into account the perspective discussed above, this study comprehensively explores the fault-tolerant synchronization of drive-response MC-NNs with the bias and effectiveness failures. The prominent contributions put forward in this paper are listed below. 1) This article comprehensively

considers two types of actuator failures within drive-response MCNNs, which are bias and effectiveness failures. 2) A bilayer fault-tolerant controller designed in this article can be directly used to achieve the synchronization of MCNNs with both bias and effectiveness failures, further minimizing network communication resource usage. The structure of this paper is outlined below. In the second part, fundamental elements such as system models, failure characterizations, and related basic concepts are introduced. The third part presents the key research findings of this paper. In the fourth part, simulation instances are provided to validate the efficacy of the proposed synchronization control strategies. Lastly, the fifth part summarizes this article and points out some future research directions.

#### 2. Model Description and Preliminaries

The memristive competitive neural networks (MCNNs) model is defined as follows:

as follows: 
$$\begin{cases} STM : \varepsilon \dot{s}_{q}(\eta) = -c_{q}s_{q}(\eta) + \sum_{l=1}^{n} h_{ql}(s_{q}(\eta))g_{l}(s_{l}(\eta)) + d_{q} \sum_{\varsigma=1}^{i} m_{q\varsigma}(\eta)v_{\varsigma}, \\ LTM : \dot{m}_{q\varsigma}(\eta) = -e_{q}m_{q\varsigma}(\eta) + b_{q}v_{\varsigma}g_{q}(s_{q}(\eta)), \end{cases}$$
(1)

where  $q=1,2,\ldots,n;\ s_q(\eta)$  serves as the current activity level of neuron;  $m_{q\varsigma}(\eta)$  indicates the synaptic adaptability,  $v_{\varsigma}$  reflects the strength of the external stimulus;  $c_q>0$  signifies the self-inhibition rate of neuron;  $g_l(\cdot)$  acts as an activation function;  $d_q>0$  represents the intensity of the external stimulus,  $\varepsilon$  denotes some time scale in STM;  $e_q>0$  and  $b_q$  are disposable scaling constants. Furthermore, the initial conditions of system (1) are:  $s_q(0)\in\mathbb{R}$ 

and  $m_{q\varsigma}(0) \in \mathbb{R}$ ;  $h_{ql}(s_q(\eta))$  acts as the synaptic connection weight of memristors, which is expressed as:

$$h_{ql}(s_q(\eta)) = \frac{\mathbb{P}_{ql}}{\mathbb{F}_q} \times \operatorname{sign}_{ql}, \ \operatorname{sign}_{ql} = \begin{cases} 1, & q \neq l, \\ -1, & q = l, \end{cases}$$

in which q, l = 1, 2, ..., n,  $\mathbb{P}_{ql}$  is designated as the memductance of memristor  $\mathbb{G}_{ql}$ , which denotes the memristor situated between  $g_l(s_l(\eta))$  and  $s_q(\eta)$ . Based on the current and voltage characteristics of the memristor, one obtains

$$h_{ql}(s_q(\eta)) = \begin{cases} \hat{h}_{ql}, & |s_q(\eta)| \leq \chi_q, \\ \check{h}_{ql}, & |s_q(\eta)| > \chi_q, \end{cases}$$

where q, l = 1, 2, ..., n,  $\hat{h}_{ql}$ ,  $\check{h}_{ql}$  represent constants,  $\chi_q > 0$  indicates the switching jumps. For convenience, we denote  $\bar{h}_{ql} = |\hat{h}_{ql} - \check{h}_{ql}|$ ,  $\tilde{h}_{ql} = \max\{|\hat{h}_{ql}|, |\check{h}_{ql}|\}$ ,  $\tilde{H} = \text{diag}(\sum_{l=1}^{n} (\tilde{h}_{1l})^2, \sum_{l=1}^{n} (\tilde{h}_{2l})^2, ..., \sum_{l=1}^{n} (\tilde{h}_{nl})^2)$ ,  $\bar{H} = (\bar{h}_{ql})_{n \times n}$ .

By defining  $||v||^2 = v_1^2 + v_2^2 + \ldots + v_i^2$  and  $M_q(\eta) = \sum_{\varsigma=1}^i m_{q\varsigma}(\eta) v_{\varsigma}$ ,  $q = 1, 2, \ldots, n$ . It is commonly assumed that the input stimulus vector v is normalized with unit magnitude  $||v||^2 = 1$  and  $\varepsilon = 1$ . Consequently, MC-NNs (1) can be rephrased as below:

$$\begin{cases}
STM : \dot{s}_{q}(\eta) = -c_{q}s_{q}(\eta) + \sum_{l=1}^{n} h_{ql}(s_{q}(\eta))g_{l}(s_{l}(\eta)) + d_{q}M_{q}(\eta), \\
LTM : \dot{M}_{q}(\eta) = -e_{q}M_{q}(\eta) + b_{q}g_{q}(s_{q}(\eta)).
\end{cases} (2)$$

Consider the above MCNNs (2) as a drive system, then the response system associated with MCNNs (2) is

$$\begin{cases}
STM : \dot{y}_{q}(\eta) = -c_{q}y_{q}(\eta) + \sum_{l=1}^{n} h_{ql}(y_{q}(\eta))g_{l}(y_{l}(\eta)) + d_{q}Q_{q}(\eta) + I_{q}^{T}K_{q}(\eta), \\
LTM : \dot{Q}_{q}(\eta) = -e_{q}Q_{q}(\eta) + b_{q}g_{q}(y_{q}(\eta)) + I_{q}^{T}W_{q}(\eta),
\end{cases} (3)$$

where  $I_q = (I_{q1}, I_{q2}, \dots, I_{q\varrho})^T \in \mathbb{R}^{\varrho}$  with  $I_{q\iota} > 0(\iota = 1, 2, \dots, \varrho)$ ; the vectors  $K_q(\eta) = (k_{q1}(\eta), k_{q2}(\eta), \dots, k_{q\varrho}(\eta))^T \in \mathbb{R}^{\varrho}$  and  $W_q(\eta) = (w_{q1}(\eta), w_{q2}(\eta), \dots, w_{q\varrho}(\eta))^T \in \mathbb{R}^{\varrho}$  are inputs that occur multiple types of potential failures.

Remark 1. In the network model of drive-response MCNNs (2) and (3), the physical properties of memristors and the competitive mechanism are integrated. Compared with traditional MNNs, MCNNs combine both the dynamic evolution of neural states and adaptive synaptic weights. This dual-layered dynamic makes MCNNs better suited to model both short-term and long-term memory processes. Moreover, the competitive mechanism among neurons enables more efficient information processing and pattern storage, which are essential for analyzing complex neural behaviors in real-world systems. In recent years, more and more scholars have focused on this kind of network and studied the dynamical behaviors of MCNNs in [31–34], such as synchronization, anti-synchronization and decay projection synchronization. However, the fault-tolerant synchronization of this type of network remains an understudied area, which forms the core motivation for the research presented in this paper.

This work simultaneously considers both bias and effectiveness failures. Actually, it has been noted in existing literatures [50–52] that the control signal acting on system (3) is formed by linearly combining the outputs of multiple actuators. However, these studies have primarily considered only actuator effectiveness failure, yet other types of failures have been overlooked. This motivates us to further explore the fault-tolerant synchronization of the MCNNs impacted by multiple actuator failures. More exactly, the models for these two kinds of actuator faults are depicted in the following manner.

The model of effectiveness failure is described by:

$$\begin{cases}
k_{q\iota}^{X}(\eta) = \beta_{q\iota}k_{q\iota}(\eta), & \eta \geqslant \hat{\eta}_{q\iota}, \\
w_{q\iota}^{X}(\eta) = \beta_{q\iota}w_{q\iota}(\eta), & \eta \geqslant \hat{\eta}_{q\iota},
\end{cases}$$
(4)

where  $\iota \in G = \{\xi | \text{the } \xi\text{-th actuator experiences the effectiveness failure}\} \subset \{1, 2, \dots, \varrho\}$ ,  $\iota$  represents the number of actuators impacted by effectiveness failures,  $k_{q\iota}^X(\eta)$  and  $w_{q\iota}^X(\eta)$  represent the output values that the actuators  $k_{q\iota}(\eta)$  and  $w_{q\iota}(\eta)$  actually produce, respectively;  $\hat{\eta}_{q\iota}$  is the occurrence time of the effectiveness failure;  $\beta_{q\iota} \in [\bar{\beta}_{q\iota}, 1]$  denotes the efficacy ratio and  $\bar{\beta}_{q\iota} > 0$  signifies the smallest value of  $\beta_{q\iota}$ .

The model of bias failure is characterized by:

$$\begin{cases}
k_{q\rho}^{V}(\eta) = \bar{k}_{q\rho}, & \eta \geqslant \check{\eta}_{q\rho}, \\
w_{q\rho}^{V}(\eta) = \bar{w}_{q\rho}, & \eta \geqslant \check{\eta}_{q\rho}.
\end{cases}$$
(5)

where  $\rho \in \bar{G} = \{\bar{\xi} | \text{the } \bar{\xi} \text{-th actuator experiences the bias failure} \} \subset \{1, 2, \cdots, \varrho\}$ ,  $\rho$  represents the number of actuators impacted by bias failures,  $k_{q\rho}^V(\eta)$  and  $w_{q\rho}^V(\eta)$  represent the output values that the actuators  $k_{q\rho}(\eta)$  and  $w_{q\rho}(\eta)$  actually produce, respectively;  $\check{\eta}_{q\rho}$  is the occurrence time of the bias failure and  $\bar{k}_{q\rho} > 0$  and  $\bar{w}_{q\rho} > 0$  are bias constants.

**Assumption 1.** (see [43]). The synchronization of drive-response systems (2) and (3) can be achieved if up to  $\varrho - 1$  actuators fail, while the remaining actuators suffer partial effectiveness loss.

With reference to the aforementioned actuator effectiveness failure model

(4) and bias failure model (5), it follows from Assumption 1 that

$$\begin{cases}
I_q^T K_q(\eta) = \sum_{\iota \in G} I_{q\iota} \beta_{q\iota} k_{q\iota}(\eta) + \sum_{\rho \in \bar{G}} I_{q\rho} \bar{k}_{q\rho}, \\
I_q^T W_q(\eta) = \sum_{\iota \in G} I_{q\iota} \beta_{q\iota} w_{q\iota}(\eta) + \sum_{\rho \in \bar{G}} I_{q\rho} \bar{w}_{q\rho}.
\end{cases} (6)$$

For the two failure models (4) and (5) mentioned above,  $\beta_{q\iota} = 1$  indicates that the actuators  $k_{q\iota}(\eta)$  and  $w_{q\iota}(\eta)$  are functioning normally, and  $\sum_{\rho\in\bar{G}}I_{q\rho}\bar{k}_{q\rho} = 0$  and  $\sum_{\rho\in\bar{G}}I_{q\rho}\bar{w}_{q\rho} = 0$  signify that the absence of bias failure in any actuator. Based on Assumption 1, it can be concluded that  $\sum_{\iota\in G}I_{q\iota}\beta_{q\iota} > 0$  holds for  $\forall \eta \geqslant 0$ .

Remark 2. In real-world engineering applications, actuators are complex electromechanical components that are prone to various failure modes. Among them, effectiveness failure and bias failure are two primary and commonly observed types. For example, the authors in [41, 42] studied effectiveness failures of actuator in their fault-tolerant synchronization strategies. However, effectiveness failure and bias failure may occur simultaneously, and they have distinct dynamic effects on the control system. More specifically, bias failures may cause constant errors that build up over time and may lead to system instability. Ignoring bias failures oversimplifies the fault model and limits the reliability and robustness of the designed controller. Furthermore, MCNNs are characterized by rich dynamics and intricate feedback mechanisms. This makes them particularly sensitive to actuator faults. Since MCNNs are widely adopted in memory computing, pattern recognition, and secure communications [31–34], where reliability and stability are critical, it is imperative to design a generalized fault model that reflects both types of

failures simultaneously. To address this gap, this work aims to systematically investigate the fault-tolerant synchronization of drive-response MCNNs with bias and effectiveness failures by designing a novel bilayer fault-tolerant controller. Note that the occurrence time and type of the actuator failures mentioned in this work are considered to have no relation with each other. Additionally, either kind of failure could occur unexpectedly and exert an influence on the system. Thus, these two types of actuator failures are both considered to better align with practical reality.

Let  $z_q(\eta) = y_q(\eta) - s_q(\eta)$  and  $\hat{z}_q(\eta) = Q_q(\eta) - M_q(\eta)$  be the error system, we obtain

we obtain
$$\begin{cases}
\dot{z}_{q}(\eta) = -c_{q}z_{q}(\eta) - (\sum_{l=1}^{n} h_{ql}(s_{q}(\eta)) - \sum_{l=1}^{n} h_{ql}(y_{q}(\eta)))g_{l}(y_{l}(\eta)) + d_{q}\hat{z}_{q}(\eta) \\
+ \sum_{l=1}^{n} h_{ql}(s_{q}(\eta))\psi_{l}(z_{l}(\eta)) + I_{q}^{T}K_{q}(\eta), \\
\dot{\hat{z}}_{q}(\eta) = -e_{q}\hat{z}_{q}(\eta) + b_{q}\psi_{q}(z_{q}(\eta)) + I_{q}^{T}W_{q}(\eta),
\end{cases} (7)$$

where  $\psi_l(z_l(\eta)) = g_l(y_l(\eta)) - g_l(s_l(\eta)).$ 

For convenience, we define  $z(\eta) = (z_1(\eta), z_2(\eta), \dots, z_n(\eta))^T$ ,  $\hat{z}(\eta) = (\hat{z}_1(\eta), z_2(\eta), \dots, \hat{z}_n(\eta))^T$ ,  $\hat{z}(\eta) = (z_1(\eta), z_2(\eta), \dots, z_n(\eta), \hat{z}_1(\eta), \hat{z}_2(\eta), \dots, \hat{z}_n(\eta))^T$ ,  $C = \text{diag}(c_1, c_2, \dots, c_n)$ ,  $C = \text{diag}(c_1, c_2, \dots, c_n)$ ,  $C = \text{diag}(d_1, d_2, \dots, d_n)$ .

**Assumption 2.** (see [44]). For any  $r, r_1, r_2 \in \mathbb{R}$ , there are positive constants  $u_l, \sigma_l, l = 1, 2, ..., n$ , such that:  $|g_l(r_1) - g_l(r_2)| \leq u_l |r_1 - r_2|$ ,  $|g_l(r)| \leq \sigma_l$ . To facilitate the demonstration given in this paper, we define  $U = \operatorname{diag}(u_1^2, u_2^2, ..., u_n^2) \in \mathbb{R}^{n \times n}$ .

**Definition 2.1.** (see [45]). For any  $\bar{z}(0) \in \mathbb{R}^{2n}$ ,  $\tau_1 > 0$  and  $\tau_2 > 0$ , if the inequality  $\|\bar{z}(\eta)\| \leq \tau_2 e^{-\tau_1(\eta-\eta_0)}$  is satisfied for  $\forall \eta \geqslant \eta_0$ , then the error network (7) is said to achieve global exponential stability.

**Definition 2.2.** (see [46]). Assume that there is a constant  $\eta^* \geq 0$  such that  $\bar{z}(\eta) = 0$  for  $\forall \eta > \eta^*$  and  $\bar{z}(0) \in \mathbb{R}^{2n}$ , then the error network (7) is said to be finite-time stable. Moreover, for  $\forall \bar{z}(0) \in \mathbb{R}^{2n}$ , the settling time function is defined as  $T(\bar{z}(0)) = \inf\{\eta^* : \bar{z}(\eta) = 0, \forall \eta > \eta^*\}$ .

**Definition 2.3.** (see [47]). The error system (7) is fixed-time stable if it satisfies finite-time stability, and there is a scalar  $T_{\text{max}} > 0$  such that  $T(\bar{z}(0)) \leq T_{\text{max}}$  for  $\forall \bar{z}(0) \in \mathbb{R}^{2n}$ . In other words, the settling time function  $T(\cdot)$  is uniformly bounded.

**Definition 2.4.** (see [48]). The error system (7) is called to be predefinedtime stable if its fixed-time stability is achieved, and for any predefined time  $T_{\delta} > 0$ , the inequality  $T(\bar{z}(0)) \leq T_{\delta}$  holds for  $\forall \bar{z}(0) \in \mathbb{R}^{2n}$ , where  $T_{\delta}$  is an adjustable parameter in the designed controller, which is irrelevant to initial value.

Remark 3. In this paper, the above-mentioned four types of synchronization differ mainly in how the convergence time is determined and controlled. Based on the definition of global exponential stability as in Definition 2.1, it is easy to know that the synchronization error decays exponentially over time. That is, the system gradually approaches the synchronized state, but the error does not become exactly zero in finite time. This approach is smooth and predictable, yet may not be fast enough for time-critical applications. According to Definition 2.2, finite-time synchronization guarantees that the

system reaches exact synchronization in a finite time, but the settling time function  $T(\bar{z}(0))$  for convergence depends on the initial conditions. This makes it difficult to determine the settling time in advance. The fixed-time synchronization introduced in Definition 2.3 improves upon finite-time synchronization by ensuring the settling time function for convergence within a uniform upper bound  $T_{\text{max}} > 0$  that is independent of the initial state. However, this bound is fixed once the system is designed and cannot be adjusted flexibly. In contrast, predefined-time synchronization, as introduced in Definition 2.4, allows users to set the desired convergence time  $T_{\delta}$  in advance. The system is then designed to synchronize within this specified time, regardless of initial conditions. This provides the highest level of flexibility, which is particularly valuable in real-time or deadline-sensitive applications.

**Lemma 2.1.** (see [45, 48, 50, 51]). Suppose there exists a function  $J(\bar{z}(\eta))$ :  $\mathbb{R}^{2n} \to \mathbb{R}^+ \cup \{0\}$ , which is continuous, positive definite and radially unbounded, such that

$$\dot{J}(\bar{z}(\eta)) \leqslant -\tau_1 J(\bar{z}(\eta)) - \tau_2 J^{\alpha_1}(\bar{z}(\eta)) - \tau_3 J^{\alpha_2}(\bar{z}(\eta))$$

then the following conclusions are established:

- 1) When  $\tau_2 = \tau_3 = 0$  and  $\tau_1 > 0$ , the error network (7) reaches global exponential stability.
- 2) When  $\tau_1 = \tau_3 = 0$ ,  $\tau_2 > 0$  and  $0 < \alpha_1 < 1$ , the error network (7) reaches finite-time stability with the corresponding time given by  $T(\bar{z}(0)) = \frac{J^{1-\alpha_1}(\bar{z}(0))}{\tau_2(1-\alpha_1)}$ .
- 3) When  $\tau_1 = 0$ ,  $\tau_2 > 0$ ,  $\tau_3 > 0$ ,  $0 < \alpha_1 < 1$  and  $\alpha_2 > 1$ , the error network (7) reaches fixed-time stability. Furthermore,  $T_{\text{max}} = \frac{1}{\tau_2(1-\alpha_1)} + \frac{1}{\tau_3(\alpha_2-1)}$ .

4) When  $\tau_1 = 0$ ,  $\tau_2 = \tau_3 = \frac{\pi}{\theta T_{\delta}} > 0$ ,  $\alpha_1 = 1 + \frac{\theta}{2} > 1$  and  $0 < \alpha_2 = 1 - \frac{\theta}{2} < 1$ , where  $0 < \theta < 1$ ,  $T_{\delta} > 0$  represents a predefined-time constant set beforehand, the error network (7) reaches predefined-time stability within the predefined-time  $T_{\delta}$ .

**Lemma 2.2.** (see [52]). If  $f_1, f_2, \dots, f_n \ge 0$ ,  $0 < \zeta_1 \le 1$ ,  $\zeta_2 > 1$ , then we have

$$\left(\sum_{q=1}^{n} f_q\right)^{\zeta_1} \leqslant \sum_{q=1}^{n} f_q^{\zeta_1}, n^{1-\zeta_2} \left(\sum_{q=1}^{n} f_q\right)^{\zeta_2} \leqslant \sum_{q=1}^{n} f_q^{\zeta_2}.$$

#### 3. Fault-tolerant synchronization of MCNNs

This section is dedicated to studying the global exponential synchronization, finite-time synchronization, fixed-time synchronization and predefinedtime synchronization problems of MCNNs through the fault-tolerant control scheme. The following theorem is presented to facilitate the synchronization of the drive-response systems (2) and (3).

**Theorem 1.** Given that Assumptions 1 and 2 are satisfied and the bilayer fault-tolerant controllers  $k_{ql}(\eta)$  and  $w_{ql}(\eta)$  for the system (7) are designed as:

$$\begin{cases} k_{ql}(\eta) = -\frac{1}{\sum_{\iota \in G} I_{q\iota} \beta_{q\iota}} \left[ \left( \delta_q^{(1)} p_q^{\varphi_1} | z_q(\eta) |^{\phi_1} + \delta_q^{(2)} p_q^{\varphi_2} | z_q(\eta) |^{\phi_2} \right) \operatorname{sign}(z_q(\eta)) \right. \\ + \sum_{l=1}^{n} \operatorname{sign}(z_q(\eta)) \bar{h}_{ql} \sigma_l + \gamma_q z_q(\eta) + \sum_{\rho \in \bar{G}} I_{q\rho} \bar{k}_{q\rho} \right], \\ w_{ql}(\eta) = -\frac{1}{\sum_{\iota \in G} I_{q\iota} \beta_{q\iota}} \left[ \left( \delta_q^{(1)} o_q^{\varphi_1} | \hat{z}_q(\eta) |^{\phi_1} + \delta_q^{(2)} o_q^{\varphi_2} | \hat{z}_q(\eta) |^{\phi_2} \right) \operatorname{sign}(\hat{z}_q(\eta)) \right. \\ + \gamma_q \hat{z}_q(\eta) + \sum_{\rho \in \bar{G}} I_{q\rho} \bar{w}_{q\rho} \right], \end{cases}$$
(8)

if there exists  $0 < P = \operatorname{diag}(p_1, p_2, \dots, p_n) \in \mathbb{R}^{n \times n}$ ,  $O = \operatorname{diag}(o_1, o_2, \dots, o_n) \in \mathbb{R}^{n \times n}$  and  $\Upsilon = \operatorname{diag}(\gamma_1, \gamma_2, \dots, \gamma_n) \in \mathbb{R}^{n \times n}$  such that

$$-2PC + P^{2}\tilde{H} + 2U + PD - 2P\Upsilon < 0, (9)$$

$$-2OE + PD + O^2B^2 - 2O\Upsilon < 0, (10)$$

then the following results are obtained.

- 1) When  $\varphi_1 = 0$ ,  $\delta_q^{(2)} = 0$ ,  $\phi_1 = 1$ ,  $\delta_q^{(1)}$ ,  $p_q$ ,  $o_q$  and  $\gamma_q$  satisfy  $\delta_q^{(1)} > 0$ ,  $p_q > 0$ ,  $o_q > 0$  and  $\gamma_q > 0$ , where  $\delta^{(1)} = \min\{\delta_q^{(1)}, q = 1, 2, \dots, n\}$ , the drive system (2) and response system (3) realize global exponential synchronization.
- 2) When  $\delta_q^{(2)} = 0$ ,  $\varphi_1 = \frac{\zeta_1 1}{2}$ ,  $\phi_1 = \zeta_1$ ,  $\delta_q^{(1)}$ ,  $p_q$ ,  $o_q$  and  $\gamma_q$  satisfy  $\delta_q^{(1)} > 0$ ,  $p_q > 0$ ,  $o_q > 0$  and  $\gamma_q > 0$ , where  $0 < \zeta_1 < 1$ ,  $\delta^{(1)} = \min\{\delta_q^{(1)}, q = 1, 2, \dots, n\}$ , the drive system (2) and response system (3) realize finite-time synchronization. Additionally,  $T(\bar{z}(0)) = \frac{J^{\frac{1-\zeta_1}{2}}(\bar{z}(0))}{\delta^{(1)}(1-\zeta_1)}$ .
- 3) When  $\varphi_1 = \frac{\zeta_1 1}{2}$ ,  $\varphi_2 = \frac{\zeta_2 1}{2}$ ,  $\phi_1 = \zeta_1$ ,  $\phi_2 = \zeta_2$ ,  $\delta_q^{(1)}$ ,  $\delta_q^{(2)}$ ,  $p_q$ ,  $o_q$  and  $\gamma_q$  satisfy  $\delta_q^{(1)} > 0$ ,  $\delta_q^{(2)} > 0$ ,  $p_q > 0$ ,  $o_q > 0$  and  $\gamma_q > 0$ , where  $0 < \zeta_1 < 1$ ,  $\zeta_2 > 1$ ,  $\delta^{(1)} = \min\{\delta_q^{(1)}, q = 1, 2, \dots, n\}$ ,  $\delta^{(2)} = \min\{\delta_q^{(2)}, q = 1, 2, \dots, n\}$ , the drive system (2) and response system (3) realize fixed-time synchronization and  $T_{\text{max}} = \frac{1}{\delta^{(1)}(1-\zeta_1)} + \frac{1}{(2n)^{\frac{1-\zeta_2}{2}}\delta^{(2)}(\zeta_2 1)}$ .
- 4) When  $\delta_q^{(1)} = \delta_1^{(1)} = \frac{\pi n^{\frac{\zeta_1}{2}}}{2^{\frac{2-\zeta_1}{2}}\zeta_1 T_{\delta}}$ ,  $\delta_q^{(2)} = \delta_1^{(2)} = \frac{\pi}{2\zeta_1 T_{\delta}}$ ,  $\varphi_1 = \frac{\zeta_1}{2}$ ,  $\varphi_2 = -\frac{\zeta_1}{2}$ ,  $\phi_1 = 1 + \zeta_1$ ,  $\phi_2 = 1 \zeta_1$ ,  $p_q$ ,  $o_q$  and  $\gamma_q$  satisfy  $p_q > 0$ ,  $o_q > 0$  and  $\gamma_q > 0$ , where  $0 < \zeta_1 < 1$ , the drive system (2) and response system (3) achieve predefined-time synchronization with predefined-time  $T_{\delta}$ .

**Proof.** Constructing the below Lyapunov functional for error system (7):

$$J(\bar{z}(\eta)) = \sum_{q=1}^{n} p_q z_q^2(\eta) + \sum_{q=1}^{n} o_q \hat{z}_q^2(\eta).$$
 (11)

The derivative of  $J(\bar{z}(\eta))$  can be calculated as

$$\dot{J}(\bar{z}(\eta)) = 2 \sum_{q=1}^{n} p_{q} z_{q}(\eta) \dot{z}_{q}(\eta) + 2 \sum_{q=1}^{n} o_{q} \hat{z}_{q}(\eta) \dot{\hat{z}}_{q}(\eta) 
= 2 \sum_{q=1}^{n} p_{q} z_{q}(\eta) \left[ -c_{q} z_{q}(\eta) + \sum_{l=1}^{n} h_{ql}(s_{q}(\eta)) \psi_{l}(z_{l}(\eta)) + d_{q} \hat{z}_{q}(\eta) + I_{q}^{T} K_{q}(\eta) \right] 
- (\sum_{l=1}^{n} h_{ql}(s_{q}(\eta)) - \sum_{l=1}^{n} h_{ql}(y_{q}(\eta))) g_{l}(y_{l}(\eta)) \right] + 2 \sum_{q=1}^{n} o_{q} \hat{z}_{q}(\eta) \left[ -e_{q} \hat{z}_{q}(\eta) + h_{q} \psi_{q}(z_{q}(\eta)) + I_{q}^{T} W_{q}(\eta) \right].$$
(12)

Apparently, one has,

$$2\sum_{q=1}^{n}\sum_{l=1}^{n}p_{q}z_{q}(\eta)h_{ql}(s_{q}(\eta))\psi_{l}(z_{l}(\eta))$$

$$\leq 2\sum_{q=1}^{n}\sum_{l=1}^{n}p_{q}|z_{q}(\eta)|\tilde{h}_{ql}|g_{l}(y_{l}(\eta)) - g_{l}(s_{l}(\eta))|$$

$$\leq 2\sum_{q=1}^{n}\sum_{l=1}^{n}p_{q}|z_{q}(\eta)|\tilde{h}_{ql}u_{l}|z_{l}(\eta)|$$

$$\leq \sum_{q=1}^{n}\sum_{l=1}^{n}p_{q}^{2}\tilde{h}_{ql}^{2}z_{q}^{2}(\eta) + \sum_{l=1}^{n}u_{l}^{2}z_{l}^{2}(\eta)$$

$$=z^{T}(\eta)(P^{2}\tilde{H} + U)z(\eta), \tag{13}$$

and

$$2\sum_{q=1}^{n} o_q \hat{z}_q(\eta) b_q \psi_q(z_q(\eta))$$

$$=2\sum_{q=1}^{n} o_{q}\hat{z}_{q}(\eta)b_{q}(g_{q}(y_{q}(\eta)) - g_{q}(s_{q}(\eta)))$$

$$\leq 2\sum_{q=1}^{n} o_{q}|\hat{z}_{q}(\eta)||b_{q}|u_{q}|z_{q}(\eta)|$$

$$\leq \sum_{q=1}^{n} o_{q}^{2}b_{q}^{2}\hat{z}_{q}^{2}(\eta) + \sum_{q=1}^{n} u_{q}^{2}z_{q}^{2}(\eta)$$

$$=\hat{z}^{T}(\eta)O^{2}B^{2}\hat{z}(\eta) + z^{T}(\eta)Uz(\eta). \tag{14}$$

Moreover,

$$-2\sum_{q=1}^{n}\sum_{l=1}^{n}p_{q}z_{q}(\eta)(h_{ql}(s_{q}(\eta)) - h_{ql}(y_{q}(\eta)))g_{l}(y_{l}(\eta))$$

$$=2\sum_{q=1}^{n}\sum_{l=1}^{n}p_{q}z_{q}(\eta)(h_{ql}(y_{q}(\eta)) - h_{ql}(s_{q}(\eta)))g_{l}(y_{l}(\eta))$$

$$\leqslant 2\sum_{q=1}^{n}\sum_{l=1}^{n}p_{q}|z_{q}(\eta)||\hat{h}_{ql} - \check{h}_{ql}||g_{l}(y_{l}(\eta))|$$

$$\leqslant 2\sum_{q=1}^{n}\sum_{l=1}^{n}p_{q}|z_{q}(\eta)|\bar{h}_{ql}\sigma_{l},$$

$$(15)$$

$$2\sum_{q=1}^{n}p_{q}z_{q}(\eta)d_{q}\hat{z}_{q}(\eta)$$

$$\leqslant 2\sum_{q=1}^{n}p_{q}d_{q}(z_{q}^{2}(\eta) + \hat{z}_{q}^{2}(\eta))$$

$$\leqslant \sum_{q=1}^{n}p_{q}d_{q}z_{q}^{2}(\eta) + \sum_{q=1}^{n}p_{q}d_{q}\hat{z}_{q}^{2}(\eta)$$

$$=z^{T}(\eta)PDz(\eta) + \hat{z}^{T}(\eta)PD\hat{z}(\eta).$$

$$(16)$$

Substituting the bilayer fault-tolerant controllers (8) into (6), we have

$$2\sum_{q=1}^{n} p_{q}z_{q}(\eta)I_{q}^{T}K_{q}(\eta)$$

$$=2\sum_{q=1}^{n} p_{q}z_{q}(\eta)\left(\sum_{\iota\in G} I_{q\iota}\beta_{q\iota}k_{q\iota}(\eta) + \sum_{\rho\in\bar{G}} I_{q\rho}\bar{k}_{q\rho}\right)$$

$$=2\sum_{q=1}^{n} p_{q}z_{q}(\eta)\left[-\left(\delta_{q}^{(1)}p_{q}^{\varphi_{1}}|z_{q}(\eta)|^{\phi_{1}} + \delta_{q}^{(2)}p_{q}^{\varphi_{2}}|z_{q}(\eta)|^{\phi_{2}}\right)\operatorname{sign}(z_{q}(\eta)) - \gamma_{q}z_{q}(\eta)\right]$$

$$-\sum_{l=1}^{n} \operatorname{sign}(z_{q}(\eta))\bar{h}_{ql}\sigma_{l} - \sum_{\rho\in\bar{G}} I_{q\rho}\bar{k}_{q\rho} + \sum_{\rho\in\bar{G}} I_{q\rho}\bar{k}_{q\rho}\right]$$

$$=-2\sum_{q=1}^{n} p_{q}z_{q}(\eta)\left[\left(\delta_{q}^{(1)}p_{q}^{\varphi_{1}}|z_{q}(\eta)|^{\phi_{1}} + \delta_{q}^{(2)}p_{q}^{\varphi_{2}}|z_{q}(\eta)|^{\phi_{2}}\right)\operatorname{sign}(z_{q}(\eta)) + \gamma_{q}z_{q}(\eta)\right]$$

$$+\sum_{l=1}^{n} \operatorname{sign}(z_{q}(\eta))\bar{h}_{ql}\sigma_{l}\right], \tag{17}$$
and

and
$$2\sum_{q=1}^{n} o_{q}\hat{z}_{q}(\eta)I_{q}^{T}W_{q}(\eta)$$

$$=2\sum_{q=1}^{n} o_{q}\hat{z}_{q}(\eta)\left(\sum_{\iota\in G} I_{q\iota}\beta_{q\iota}w_{q\iota}(\eta) + \sum_{\rho\in\bar{G}} I_{q\rho}\bar{w}_{q\rho}\right)$$

$$=2\sum_{q=1}^{n} o_{q}\hat{z}_{q}(\eta)\left[-\left(\delta_{q}^{(1)}o_{q}^{\varphi_{1}}|\hat{z}_{q}(\eta)|^{\phi_{1}} + \delta_{q}^{(2)}o_{q}^{\varphi_{2}}|\hat{z}_{q}(\eta)|^{\phi_{2}}\right)\operatorname{sign}(\hat{z}_{q}(\eta)) - \gamma_{q}\hat{z}_{q}(\eta)$$

$$-\sum_{\rho\in\bar{G}} I_{q\rho}\bar{w}_{q\rho} + \sum_{\rho\in\bar{G}} I_{q\rho}\bar{w}_{q\rho}\right]$$

$$=-2\sum_{q=1}^{n} o_{q}\hat{z}_{q}(\eta)\left[\left(\delta_{q}^{(1)}o_{q}^{\varphi_{1}}|\hat{z}_{q}(\eta)|^{\phi_{1}} + \delta_{q}^{(2)}o_{q}^{\varphi_{2}}|\hat{z}_{q}(\eta)|^{\phi_{2}}\right)\operatorname{sign}(\hat{z}_{q}(\eta)) + \gamma_{q}\hat{z}_{q}(\eta)\right]. (18)$$

Substituting (13) - (18) into (12), then we have

$$\dot{J}(\bar{z}(\eta)) \leqslant z^{T}(\eta) \left[ -2PC + P^{2}\tilde{H} + 2U + PD - 2P\Upsilon \right] z(\eta) + \hat{z}^{T}(\eta) \left[ -2OE \right] z(\eta) + \hat{z}^{T}(\eta) + \hat{z}^{T}($$

$$+ PD + O^{2}B^{2} - 2O\Upsilon) \hat{z}(\eta) - 2 \sum_{q=1}^{n} p_{q} z_{q}(\eta) \Big[ \left( \delta_{q}^{(1)} p_{q}^{\varphi_{1}} | z_{q}(\eta) |^{\phi_{1}} \right) \\ + \delta_{q}^{(2)} p_{q}^{\varphi_{2}} | z_{q}(\eta) |^{\phi_{2}} \Big] \operatorname{sign}(z_{q}(\eta)) \Big] - 2 \sum_{q=1}^{n} o_{q} \hat{z}_{q}(\eta) \Big[ \left( \delta_{q}^{(1)} o_{q}^{\varphi_{1}} | \hat{z}_{q}(\eta) |^{\phi_{1}} \right) \\ + \delta_{q}^{(2)} o_{q}^{\varphi_{2}} | \hat{z}_{q}(\eta) |^{\phi_{2}} \Big) \operatorname{sign}(\hat{z}_{q}(\eta)) \Big].$$

Thereafter, we will discuss the impact of the controller variables on the stability of the system (7).

Case 1: Based on the variable conditions of Case 1, and applying Lemma 2.2, we get

$$-2\sum_{q=1}^{n} p_{q}z_{q}(\eta) \left[ \left( \delta_{q}^{(1)} p_{q}^{\varphi_{1}} | z_{q}(\eta) |^{\phi_{1}} + \delta_{q}^{(2)} p_{q}^{\varphi_{2}} | z_{q}(\eta) |^{\phi_{2}} \right) \operatorname{sign}(z_{q}(\eta)) \right]$$

$$= -2\sum_{q=1}^{n} \delta_{q}^{(1)} p_{q}z_{q}(\eta) \operatorname{sign}(z_{q}(\eta)) |z_{q}(\eta)|$$

$$\leq -2\delta^{(1)} \sum_{q=1}^{n} p_{q}z_{q}^{2}(\eta),$$

$$-2\sum_{q=1}^{n} o_{q}\hat{z}_{q}(\eta) \left[ \left( \delta_{q}^{(1)} o_{q}^{\varphi_{1}} |\hat{z}_{q}(\eta)|^{\phi_{1}} + \delta_{q}^{(2)} o_{q}^{\varphi_{2}} |\hat{z}_{q}(\eta)|^{\phi_{2}} \right) \operatorname{sign}(\hat{z}_{q}(\eta)) \right]$$

$$= -2\sum_{q=1}^{n} \delta_{q}^{(1)} o_{q}\hat{z}_{q}(\eta) \operatorname{sign}(\hat{z}_{q}(\eta)) |\hat{z}_{q}(\eta)|$$

$$\leq -2\delta^{(1)} \sum_{q=1}^{n} o_{q}\hat{z}_{q}^{2}(\eta).$$

Based on the preceding analysis, we can conclude the following:

$$\begin{split} \dot{J}(\bar{z}(\eta)) \leqslant & z^T(\eta) \big[ -2PC + P^2 \tilde{H} + 2U + PD - 2P\Upsilon \big] z(\eta) + \hat{z}^T(\eta) \big[ -2OE \\ & + PD + O^2 B^2 - 2O\Upsilon) \big] \hat{z}(\eta) - 2\delta^{(1)} \sum_{q=1}^n p_q z_q^2(\eta) - 2\delta^{(1)} \sum_{q=1}^n o_q \hat{z}_q^2(\eta) \end{split}$$

$$\leq -2\delta^{(1)} \left( \sum_{q=1}^{n} p_q z_q^2(\eta) + \sum_{q=1}^{n} o_q \hat{z}_q^2(\eta) \right)$$

$$= -2\delta^{(1)} J(\bar{z}(\eta)).$$

According to Lemma 2.1, it follows that the error system (7) achieves global exponential synchronization when the bilayer fault-tolerant controller (8) is applied under the parameter conditions given in Case 1.

Case 2: Considering the variable conditions in Case 2, and by way of Lemma 2.2, one gets

$$\begin{split} &-2\sum_{q=1}^{n}p_{q}z_{q}(\eta)\left[\left(\delta_{q}^{(1)}p_{q}^{\varphi_{1}}|z_{q}(\eta)|^{\phi_{1}}+\delta_{q}^{(2)}p_{q}^{\varphi_{2}}|z_{q}(\eta)|^{\phi_{2}}\right)\mathrm{sign}(z_{q}(\eta))\right]\\ &=-2\sum_{q=1}^{n}\delta_{q}^{(1)}p_{q}^{\frac{1+\zeta_{1}}{2}}z_{q}(\eta)\mathrm{sign}(z_{q}(\eta))|z_{q}(\eta)|^{\zeta_{1}}\\ &\leqslant-2\delta^{(1)}\sum_{q=1}^{n}p_{q}^{\frac{1+\zeta_{1}}{2}}|z_{q}(\eta)|^{1+\zeta_{1}}\\ &\leqslant-2\delta^{(1)}\left(\sum_{q=1}^{n}p_{q}z_{q}^{2}(\eta)\right)^{\frac{1+\zeta_{1}}{2}}, \end{split}$$

and

$$\begin{split} & -2\sum_{q=1}^{n}o_{q}\hat{z}_{q}(\eta)\left[\left(\delta_{q}^{(1)}o_{q}^{\varphi_{1}}|\hat{z}_{q}(\eta)|^{\phi_{1}}+\delta_{q}^{(2)}o_{q}^{\varphi_{2}}|\hat{z}_{q}(\eta)|^{\phi_{2}}\right)\mathrm{sign}(\hat{z}_{q}(\eta))\right] \\ & = -2\sum_{q=1}^{n}\delta_{q}^{(1)}o_{q}^{\frac{1+\zeta_{1}}{2}}\hat{z}_{q}(\eta)\mathrm{sign}(\hat{z}_{q}(\eta))|\hat{z}_{q}(\eta)|^{\zeta_{1}} \\ & \leqslant -2\delta^{(1)}\sum_{q=1}^{n}o_{q}^{\frac{1+\zeta_{1}}{2}}|\hat{z}_{q}(\eta)|^{1+\zeta_{1}} \\ & \leqslant -2\delta^{(1)}\left(\sum_{q=1}^{n}o_{q}\hat{z}_{q}^{2}(\eta)\right)^{\frac{1+\zeta_{1}}{2}}. \end{split}$$

From the preceding analysis, the following conclusions can be drawn:

$$\begin{split} \dot{J}(\bar{z}(\eta)) &\leqslant z^T(\eta) \big[ -2PC + P^2 \tilde{H} + 2U + PD - 2P\Upsilon \big] z(\eta) + \hat{z}^T(\eta) \big[ -2OE + PD \\ &+ O^2 B^2 - 2O\Upsilon) \big] \hat{z}(\eta) - 2\delta^{(1)} \left( \sum_{q=1}^n p_q z_q^2(\eta) \right)^{\frac{1+\zeta_1}{2}} - 2\delta^{(1)} \left( \sum_{q=1}^n o_q \hat{z}_q^2(\eta) \right)^{\frac{1+\zeta_1}{2}} \\ &\leqslant -2\delta^{(1)} \left[ \left( \sum_{q=1}^n p_q z_q^2(\eta) \right)^{\frac{1+\zeta_1}{2}} + \left( \sum_{q=1}^n o_q \hat{z}_q^2(\eta) \right)^{\frac{1+\zeta_1}{2}} \right] \\ &\leqslant -2\delta^{(1)} \left( \sum_{q=1}^n p_q z_q^2(\eta) + \sum_{q=1}^n o_q \hat{z}_q^2(\eta) \right)^{\frac{1+\zeta_1}{2}} \\ &= -2\delta^{(1)} \left( J(\bar{z}(\eta)) \right)^{\frac{1+\zeta_1}{2}}. \end{split}$$

According to Lemma 2.1, the error network (7) reaches globally finite-time synchronization, and  $T(\bar{z}(0)) = \frac{J^{\frac{1-\zeta_1}{2}}(\bar{z}(0))}{\delta^{(1)}(1-\zeta_1)}$ .

Case 3: Taking into account the variable conditions in Case 3, one has

$$\begin{split} &-2\sum_{q=1}^{n}p_{q}z_{q}(\eta)\left[\left(\delta_{q}^{(1)}p_{q}^{\varphi_{1}}|z_{q}(\eta)|^{\phi_{1}}+\delta_{q}^{(2)}p_{q}^{\varphi_{2}}|z_{q}(\eta)|^{\phi_{2}}\right)\mathrm{sign}(z_{q}(\eta))\right]\\ &=-2\sum_{q=1}^{n}\delta_{q}^{(1)}p_{q}^{\frac{1+\zeta_{1}}{2}}z_{q}(\eta)\mathrm{sign}(z_{q}(\eta))|z_{q}(\eta)|^{\zeta_{1}}\\ &-2\sum_{q=1}^{n}\delta_{q}^{(2)}p_{q}^{\frac{1+\zeta_{2}}{2}}z_{q}(\eta)\mathrm{sign}(z_{q}(\eta))|z_{q}(\eta)|^{\zeta_{2}}\\ &=-2\sum_{q=1}^{n}\delta_{q}^{(1)}p_{q}^{\frac{1+\zeta_{1}}{2}}|z_{q}(\eta)|^{1+\zeta_{1}}-2\sum_{q=1}^{n}\delta_{q}^{(2)}p_{q}^{\frac{1+\zeta_{2}}{2}}|z_{q}(\eta)|^{1+\zeta_{2}}\\ &\leqslant-2\delta^{(1)}\sum_{q=1}^{n}p_{q}^{\frac{1+\zeta_{1}}{2}}|z_{q}(\eta)|^{1+\zeta_{1}}-2\delta^{(2)}\sum_{q=1}^{n}p_{q}^{\frac{1+\zeta_{2}}{2}}|z_{q}(\eta)|^{1+\zeta_{2}}\\ &\leqslant-2\delta^{(1)}\left(\sum_{q=1}^{n}p_{q}z_{q}^{2}(\eta)\right)^{\frac{1+\zeta_{1}}{2}}-2\delta^{(2)}n^{\frac{1-\zeta_{2}}{2}}\left(\sum_{q=1}^{n}p_{q}z_{q}^{2}(\eta)\right)^{\frac{1+\zeta_{2}}{2}}. \end{split}$$

Similarly.

$$-2\sum_{q=1}^{n}o_{q}\hat{z}_{q}(\eta)\left[\left(\delta_{q}^{(1)}o_{q}^{\varphi_{1}}|\hat{z}_{q}(\eta)|^{\phi_{1}}+\delta_{q}^{(2)}o_{q}^{\varphi_{2}}|\hat{z}_{q}(\eta)|^{\phi_{2}}\right)\operatorname{sign}(\hat{z}_{q}(\eta))\right]$$

$$=-2\sum_{q=1}^{n}\delta_{q}^{(1)}o_{q}^{\frac{1+\zeta_{1}}{2}}\hat{z}_{q}(\eta)\operatorname{sign}(\hat{z}_{q}(\eta))|\hat{z}_{q}(\eta)|^{\zeta_{1}}$$

$$-2\sum_{q=1}^{n}\delta_{q}^{(2)}o_{q}^{\frac{1+\zeta_{2}}{2}}\hat{z}_{q}(\eta)\operatorname{sign}(\hat{z}_{q}(\eta))|\hat{z}_{q}(\eta)|^{\zeta_{2}}$$

$$\leq-2\delta^{(1)}\left(\sum_{q=1}^{n}o_{q}\hat{z}_{q}^{2}(\eta)\right)^{\frac{1+\zeta_{1}}{2}}-2\delta^{(2)}n^{\frac{1-\zeta_{2}}{2}}\left(\sum_{q=1}^{n}o_{q}\hat{z}_{q}^{2}(\eta)\right)^{\frac{1+\zeta_{2}}{2}}.$$

According to analyses presented above,

$$\begin{split} \dot{J}(\eta) \leqslant &z^T(\eta) \big[ -2PC + P^2 \tilde{H} + 2U + PD - 2P\Upsilon \big] z(\eta) + \hat{z}^T(\eta) \big[ -2OE + PD \\ &+ O^2 B^2 - 2O\Upsilon \big] \big] \hat{z}(\eta) - 2\delta^{(1)} \left( \sum_{q=1}^n p_q z_q^2(\eta) \right)^{\frac{1+\zeta_1}{2}} - 2\delta^{(1)} \left( \sum_{q=1}^n o_q \hat{z}_q^2(\eta) \right)^{\frac{1+\zeta_1}{2}} \\ &- 2\delta^{(2)} n^{\frac{1-\zeta_2}{2}} \left( \sum_{q=1}^n p_q z_q^2(\eta) \right)^{\frac{1+\zeta_1}{2}} - 2\delta^{(2)} n^{\frac{1-\zeta_2}{2}} \left( \sum_{q=1}^n o_q \hat{z}_q^2(\eta) \right)^{\frac{1+\zeta_1}{2}} \\ \leqslant &- 2\delta^{(1)} \left[ \left( \sum_{q=1}^n p_q z_q^2(\eta) \right)^{\frac{1+\zeta_1}{2}} + \left( \sum_{q=1}^n o_q \hat{z}_q^2(\eta) \right)^{\frac{1+\zeta_1}{2}} \right] \\ &- 2\delta^{(2)} n^{\frac{1-\zeta_2}{2}} \left[ \left( \sum_{q=1}^n p_q z_q^2(\eta) \right)^{\frac{1+\zeta_1}{2}} + \left( \sum_{q=1}^n o_q \hat{z}_q^2(\eta) \right)^{\frac{1+\zeta_1}{2}} \right] \\ \leqslant &- 2\delta^{(1)} \left( \sum_{q=1}^n p_q z_q^2(\eta) + \sum_{q=1}^n o_q \hat{z}_q^2(\eta) \right)^{\frac{1+\zeta_1}{2}} - 2(2n)^{\frac{1-\zeta_2}{2}} \delta^{(2)} \left( \int_{q=1}^n p_q z_q^2(\eta) \right)^{\frac{1+\zeta_1}{2}} \\ &+ \sum_{q=1}^n o_q \hat{z}_q^2(\eta) \right)^{\frac{1+\zeta_1}{2}} - 2(2n)^{\frac{1-\zeta_2}{2}} \delta^{(2)} \left( J(\bar{z}(\eta)) \right)^{\frac{1+\zeta_2}{2}}. \end{split}$$

According to Lemma 2.1, the drive and response systems (2) and (3) achieve fixed-time synchronization within a fixed settling time  $T_{\text{max}} = \frac{1}{\delta^{(1)}(1-\zeta_1)} +$ 

$$\frac{1}{(2n)^{\frac{1-\zeta_2}{2}}\delta^{(2)}(\zeta_2-1)}.$$

Case 4: Referring to the previously discuss, it is evident that

$$\begin{split} &-2\sum_{q=1}^{n}p_{q}z_{q}(\eta)\left[\left(\delta_{q}^{(1)}p_{q}^{\varphi_{1}}|z_{q}(\eta)|^{\phi_{1}}+\delta_{q}^{(2)}p_{q}^{\varphi_{2}}|z_{q}(\eta)|^{\phi_{2}}\right)\mathrm{sign}(z_{q}(\eta))\right]\\ &=-2\sum_{q=1}^{n}\delta_{q}^{(1)}p_{q}^{1+\frac{\zeta_{1}}{2}}z_{q}(\eta)\mathrm{sign}(z_{q}(\eta))|z_{q}(\eta)|^{1+\zeta_{1}}\\ &-2\sum_{q=1}^{n}\delta_{q}^{(2)}p_{q}^{1-\frac{\zeta_{1}}{2}}z_{q}(\eta)\mathrm{sign}(z_{q}(\eta))|z_{q}(\eta)|^{1-\zeta_{1}}\\ &=-2\delta_{1}^{(1)}\sum_{q=1}^{n}p_{q}^{1+\frac{\zeta_{1}}{2}}|z_{q}(\eta)|^{2+\zeta_{1}}-2\delta_{1}^{(2)}\sum_{q=1}^{n}p_{q}^{1-\frac{\zeta_{1}}{2}}|z_{q}(\eta)|^{2-\zeta_{1}}\\ &\leqslant-2\frac{\delta_{1}^{(1)}}{n^{\frac{\zeta_{1}}{2}}}\left(\sum_{q=1}^{n}p_{q}z_{q}^{2}(\eta)\right)^{1+\frac{\zeta_{1}}{2}}-2\delta_{1}^{(2)}\left(\sum_{q=1}^{n}p_{q}z_{q}^{2}(\eta)\right)^{1-\frac{\zeta_{1}}{2}}.\end{split}$$
 milarly,

Similarly,

$$-2\sum_{q=1}^{n}o_{q}\hat{z}_{q}(\eta)\left[\left(\delta_{q}^{(1)}o_{q}^{\varphi_{1}}|\hat{z}_{q}(\eta)|^{\phi_{1}}+\delta_{q}^{(2)}o_{q}^{\varphi_{2}}|\hat{z}_{q}(\eta)|^{\phi_{2}}\right)\operatorname{sign}(\hat{z}_{q}(\eta))\right]$$

$$=-2\sum_{q=1}^{n}\delta_{q}^{(1)}o_{q}^{1+\frac{\zeta_{1}}{2}}\hat{z}_{q}(\eta)\operatorname{sign}(\hat{z}_{q}(\eta))|\hat{z}_{q}(\eta)|^{1+\zeta_{1}}$$

$$-2\sum_{q=1}^{n}\delta_{q}^{(2)}o_{q}^{1-\frac{\zeta_{1}}{2}}\hat{z}_{q}(\eta)\operatorname{sign}(\hat{z}_{q}(\eta))|\hat{z}_{q}(\eta)|^{1-\zeta_{1}}$$

$$\leqslant -2\frac{\delta_{1}^{(1)}}{n^{\frac{\zeta_{1}}{2}}}\left(\sum_{q=1}^{n}o_{q}\hat{z}_{q}^{2}(\eta)\right)^{1+\frac{\zeta_{1}}{2}}-2\delta_{1}^{(2)}\left(\sum_{q=1}^{n}o_{q}\hat{z}_{q}^{2}(\eta)\right)^{1-\frac{\zeta_{1}}{2}}.$$

According to analyses presented above,

$$\dot{J}(\bar{z}(\eta)) \leqslant z^T(\eta) \left[ -2PC + P^2 \tilde{H} + 2U + PD - 2P\Upsilon \right] z(\eta) + \hat{z}^T(\eta) \left[ -2OE + PD - 2P\Upsilon \right] z(\eta) + \hat{z}^T(\eta) \left[ -2OE + PD - 2P\Upsilon \right] z(\eta) + \hat{z}^T(\eta) \left[ -2DE + PD - 2D\Upsilon \right] z(\eta) + \hat{z}^T(\eta) +$$

$$\begin{split} &+O^2B^2-2O\Upsilon)\big]\hat{z}(\eta)-2\frac{\delta_{1}^{(1)}}{n^{\frac{\zeta_{1}}{2}}}\left(\sum_{q=1}^{n}p_{q}z_{q}^{2}(\eta)\right)^{1+\frac{\zeta_{1}}{2}} \\ &-2\delta_{1}^{(1)}\left(\sum_{q=1}^{n}p_{q}z_{q}^{2}(\eta)\right)^{1+\frac{\zeta_{1}}{2}} \\ &-2\delta_{1}^{(2)}\left(\sum_{q=1}^{n}p_{q}z_{q}^{2}(\eta)\right)^{1+\frac{\zeta_{1}}{2}} \\ &\leqslant -2\frac{\delta_{1}^{(1)}}{n^{\frac{\zeta_{1}}{2}}}\left[\left(\sum_{q=1}^{n}p_{q}z_{q}^{2}(\eta)\right)^{1+\frac{\zeta_{1}}{2}} + \left(\sum_{q=1}^{n}o_{q}\hat{z}_{q}^{2}(\eta)\right)^{1+\frac{\zeta_{1}}{2}}\right] \\ &-2\delta_{1}^{(2)}\left[\left(\sum_{q=1}^{n}p_{q}z_{q}^{2}(\eta)\right)^{1-\frac{\zeta_{1}}{2}} + \left(\sum_{q=1}^{n}o_{q}\hat{z}_{q}^{2}(\eta)\right)^{1+\frac{\zeta_{1}}{2}}\right] \\ &\leqslant -\frac{2^{\frac{2-\zeta_{1}}{2}}\delta_{1}^{(1)}}{n^{\frac{\zeta_{1}}{2}}}\left(\sum_{q=1}^{n}p_{q}z_{q}^{2}(\eta) + \sum_{q=1}^{n}o_{q}\hat{z}_{q}^{2}(\eta)\right)^{1+\frac{\zeta_{1}}{2}} - 2\delta_{1}^{(2)}\left(\sum_{q=1}^{n}p_{q}z_{q}^{2}(\eta) + \sum_{q=1}^{n}o_{q}\hat{z}_{q}^{2}(\eta)\right)^{1-\frac{\zeta_{1}}{2}} \\ &+ \sum_{q=1}^{n}o_{q}\hat{z}_{q}^{2}(\eta)\right)^{1-\frac{\zeta_{1}}{2}} \\ &= -\frac{2^{\frac{2-\zeta_{1}}{2}}\delta_{1}^{(1)}}{n^{\frac{\zeta_{1}}{2}}}\left(J(\bar{z}(\eta))\right)^{1+\frac{\zeta_{1}}{2}} - 2\delta_{1}^{(2)}\left(J(\bar{z}(\eta))\right)^{1-\frac{\zeta_{1}}{2}} \\ &= -\frac{\pi}{\zeta_{1}T_{h}}\big[\left(J(\bar{z}(\eta))\right)^{1+\frac{\zeta_{1}}{2}} + \left(J(\bar{z}(\eta))\right)^{1-\frac{\zeta_{1}}{2}}\big], \end{split}$$

where  $\delta_q^{(1)} = \delta_1^{(1)} = \frac{\pi n^{\frac{\zeta_1}{2}}}{2^{\frac{2-\zeta_1}{2}}\zeta_1 T_{\delta}}$ ,  $\delta_q^{(2)} = \delta_1^{(2)} = \frac{\pi}{2\zeta_1 T_{\delta}}$ . Based on Lemma 2.1, the error system (7) achieves predefined-time synchronization within predefined-time  $T_{\delta}$  by applying the bilayer fault-tolerant controllers (8).

Remark 4. As is well known, CNNs considered in this paper usually are composed of two types of state variables including STM and LTM, where STM reflects rapidly changing dynamics of neurons while LTM represents slow activities of unsupervised synaptic modifications. Since CNNs have two distinct time scales, it can handle information through inhibition, competi-

tion, coordination, and excitation between neurons. Therefore, this class of network has great application value in image processing, modern biomedicine, optimization and especially secure communication. Recently, some meaningful results on dynamics of CNNs have been published [21–26]. On the other hand, memristive NNs are able to simulate the human brain in a better way via replacing the traditional resistor with memristor. By integrating memristive characteristics into CNNs, MCNNs can be constructed. Taking into account their advantages in practical applications, some scholars have begun to study dynamics of MCNNs [31–34]. However, these studies did not consider actuator failures commonly encountered in practical control systems, such as effectiveness failure and bias failure. This has thus motivated us to develop an efficient fault-tolerant control strategy in this paper, aiming to achieve synchronization of MCNNs under multiple actuator faults. To the best of our knowledge, this marks the first step in exploring fault-tolerant synchronization of MCNNs subject to multiple actuator failures.

Remark 5. It is worth emphasizing that the conditions (9) and (10) given in Theorem 1 acts as the sufficient conditions for achieving fault-tolerant synchronization of MCNNs (7). To be more precise, the fault-tolerant synchronization of the considered network can be achieved under the well-designed bilayer fault-tolerant controllers (8) if there exist three matrices P, O and  $\Upsilon$  that satisfy the matrix inequality conditions (9) and (10). Essentially, the conditions in this theorem exhibits relatively low conservatism, which is attributed to the presence of the positive definite diagonal matrices P and O in this theorem. In numerous existing studies, the quadratic term of Lyapunov functionals typically omits the positive weighting coefficients, instead

adopting a simple sum-of-squares form of error state variables. By contrast, our two quadratic terms targeting two error components of STM and LTM in Lyapunov functional (11) incorporate two sets of positive constants  $p_q$  and  $o_q$ , which forms two positive definite diagonal matrices P and O. Compared with the traditional Lyapunov functional forms that exclude positive constants, our design reduces conservatism to a certain extent, thereby improving the flexibility of the derived fault-tolerant synchronization conditions in Theorem 1.

**Remark 6.** The fault-tolerant synchronization technique proposed in this paper boasts distinct advantages and holds substantial significance for research on the synchronization of MCNNs. A general bilayer fault-tolerant controller (8) is designed, and by assigning distinct parameter values to this controller, four types of synchronization criteria for MCNNs – specifically global exponential, finite-time, fixed-time, and predefined-time synchronization – are established accordingly. Among these, the predefined-time synchronization of drive-response MCNNs achieves the most precise and controllable performance. In contrast to other synchronization strategies, the predefined-time method ensures synchronization within a predefined-time  $T_{\delta}$  irrespective of initial conditions, which is particularly valuable for timecritical applications such as secure communications and safety-critical automation systems. It is worth noting that applying a fault-tolerant control strategy to achieve synchronization of MCNNs under multiple actuator failures constitutes a novel approach, which offers greater flexibility and adaptability in comparison to traditional methods.

#### 4. Numerical examples

Consider the following drive and response MCNNs:

$$\begin{cases}
STM : \dot{s}_{q}(\eta) = -c_{q}s_{q}(\eta) + \sum_{l=1}^{6} h_{ql}(s_{q}(\eta))g_{l}(s_{l}(\eta)) + d_{q}M_{q}(\eta), \\
LTM : \dot{M}_{q}(\eta) = -e_{q}M_{q}(\eta) + b_{q}g_{q}(s_{q}(\eta)),
\end{cases} (19)$$

$$\begin{cases}
STM : \dot{s}_{q}(\eta) = -c_{q}s_{q}(\eta) + \sum_{l=1}^{6} h_{ql}(s_{q}(\eta))g_{l}(s_{l}(\eta)) + d_{q}M_{q}(\eta), \\
LTM : \dot{M}_{q}(\eta) = -e_{q}M_{q}(\eta) + b_{q}g_{q}(s_{q}(\eta)),
\end{cases}$$
and
$$\begin{cases}
STM : \dot{y}_{q}(\eta) = -c_{q}y_{q}(\eta) + \sum_{l=1}^{6} h_{ql}(y_{q}(\eta))g_{l}(y_{l}(\eta)) + d_{q}Q_{q}(\eta) + I_{q}^{T}K_{q}(\eta), \\
LTM : \dot{Q}_{q}(\eta) = -e_{q}Q_{q}(\eta) + b_{q}g_{q}(y_{q}(\eta)) + I_{q}^{T}W_{q}(\eta),
\end{cases}$$
(20)

where  $q = 1, 2, ..., 6, g_i(a) = \frac{|a+1|+|a-1|}{5} (i = 1, 2, ..., 6), C = diag(0.5, 0.7, 0.9, 6)$ 1.3),  $D = \text{diag}(0.4, 0.2, 0.6, 0.5, 0.9, 0.3), I_1 = I_2 = I_3 = I_4 = I_5 = I_6 = I_6 = I_8 = I_8$  $[1,1,1,1,1,1]^T$ . The parameters in actuator failures are taken as  $\bar{k}_{11}=0.4$ ,  $\bar{k}_{12}=0.3,\ \bar{k}_{13}=0.5,\ \bar{w}_{11}=0.5,\ \bar{w}_{12}=0.2,\ \bar{w}_{13}=0.9,\ \beta_{14}=0.5,\ \beta_{15}=0.3,$  $\beta_{16} = 0.9, \ \bar{k}_{21} = 0.2, \ \bar{k}_{22} = 0.6, \ \bar{k}_{23} = 0.4, \ \bar{w}_{21} = 0.3, \ \bar{w}_{22} = 0.6, \ \bar{w}_{23} = 0.4,$  $\beta_{24} = 0.6, \ \beta_{25} = 0.4, \ \beta_{26} = 0.3, \ \bar{k}_{31} = 0.5, \ \bar{k}_{32} = 0.7, \ \bar{k}_{33} = 0.3, \ \bar{w}_{31} = 0.4,$  $\bar{w}_{32} = 0.8, \ \bar{w}_{\bar{3}\bar{3}} = 0.3, \ \beta_{34} = 0.2, \ \beta_{35} = 0.5, \ \beta_{36} = 0.8, \ \bar{k}_{41} = 0.6, \ \bar{k}_{42} = 0.8,$  $\bar{k}_{43} = 0.7, \ \bar{w}_{41} = 0.6, \ \bar{w}_{42} = 0.7, \ \bar{w}_{43} = 0.8, \ \beta_{44} = 0.9, \ \beta_{45} = 0.7, \ \beta_{46} = 0.4,$  $\bar{k}_{51} = 0.3, \ \bar{k}_{52} = 0.4, \ \bar{k}_{53} = 0.6, \ \bar{w}_{51} = 0.9, \ \bar{w}_{52} = 0.3, \ \bar{w}_{53} = 0.6, \ \beta_{54} = 0.8,$  $\beta_{55} \, = \, 0.6, \; \beta_{56} \, = \, 0.5, \; \bar{k}_{61} \, = \, 0.7, \; \bar{k}_{62} \, = \, 0.5, \; \bar{k}_{63} \, = \, 0.8, \; \bar{w}_{61} \, = \, 0.7, \; \bar{w}_{62} \, = \, 0.4, \; \bar{w}_{61} \, = \, 0.7, \; \bar{w}_{62} \, = \, 0.4, \; \bar{w}_{63} \, = \, 0.8, \; \bar{w}_{61} \, = \, 0.7, \; \bar{w}_{62} \, = \, 0.4, \; \bar{w}_{63} \, = \, 0.8, \; \bar{w}_{61} \, = \, 0.7, \; \bar{w}_{62} \, = \, 0.4, \; \bar{w}_{63} \, = \, 0.8, \; \bar{w}_{61} \, = \, 0.7, \; \bar{w}_{62} \, = \, 0.4, \; \bar{w}_{63} \, = \, 0.8, \; \bar{w}_{61} \, = \, 0.7, \; \bar{w}_{62} \, = \, 0.4, \; \bar{w}_{63} \, = \, 0.8, \; \bar{w}_{61} \, = \, 0.7, \; \bar{w}_{62} \, = \, 0.4, \; \bar{w}_{63} \, = \, 0.8, \; \bar{w}_{61} \, = \, 0.7, \; \bar{w}_{62} \, = \, 0.4, \; \bar{w}_{63} \, = \, 0.8, \; \bar{w}_{61} \, = \, 0.7, \; \bar{w}_{62} \, = \, 0.4, \; \bar{w}_{63} \, = \, 0.8, \; \bar{w}_{61} \, = \, 0.7, \; \bar{w}_{62} \, = \, 0.4, \; \bar{w}_{63} \, = \, 0.8, \; \bar{w}_{61} \, = \, 0.7, \; \bar{w}_{62} \, = \, 0.4, \; \bar{w}_{63} \, = \, 0.8, \; \bar{w}_{61} \, = \, 0.7, \; \bar{w}_{62} \, = \, 0.4, \; \bar{w}_{63} \, = \, 0.8, \; \bar{w}_{61} \, = \, 0.7, \; \bar{w}_{62} \, = \, 0.4, \; \bar{w}_{63} \, = \, 0.8, \; \bar{w$  $\bar{w}_{63} = 0.5, \, \beta_{64} = 0.4, \, \beta_{65} = 0.9, \, \beta_{66} = 0.6.$  The synaptic connection weight of memristors  $h_{ql}(s_q(\eta))$  is designed as follows:

$$h_{11}(s_1(\eta)) = \begin{cases} -0.22, & |s_1(\eta)| \le 0.9, \\ 0.50, & |s_1(\eta)| > 0.9, \end{cases} \quad h_{12}(s_1(\eta)) = \begin{cases} -0.48, & |s_1(\eta)| \le 0.9, \\ -0.32, & |s_1(\eta)| > 0.9, \end{cases}$$

$$\begin{split} h_{13}(s_1(\eta)) &= \begin{cases} -0.13, & |s_1(\eta)| \leqslant 0.9, \\ 0.53, & |s_1(\eta)| > 0.9, \end{cases} & h_{14}(s_1(\eta)) &= \begin{cases} -0.20, & |s_1(\eta)| \leqslant 0.9, \\ 0.52, & |s_1(\eta)| > 0.9, \end{cases} \\ h_{15}(s_1(\eta)) &= \begin{cases} -0.47, & |s_1(\eta)| \leqslant 0.9, \\ -0.30, & |s_1(\eta)| > 0.9, \end{cases} & h_{16}(s_1(\eta)) &= \begin{cases} -0.14, & |s_1(\eta)| \leqslant 0.9, \\ 0.51, & |s_1(\eta)| > 0.9, \end{cases} \\ h_{21}(s_2(\eta)) &= \begin{cases} -0.51, & |s_2(\eta)| \leqslant 0.9, \\ -0.38, & |s_2(\eta)| > 0.9, \end{cases} & h_{22}(s_2(\eta)) &= \begin{cases} 0.44, & |s_2(\eta)| \leqslant 0.9, \\ 0.26, & |s_2(\eta)| > 0.9, \end{cases} \\ h_{23}(s_2(\eta)) &= \begin{cases} 0.42, & |s_2(\eta)| \leqslant 0.9, \\ -0.52, & |s_2(\eta)| > 0.9, \end{cases} & h_{24}(s_2(\eta)) &= \begin{cases} -0.54, & |s_2(\eta)| \leqslant 0.9, \\ -0.37, & |s_2(\eta)| > 0.9, \end{cases} \\ h_{25}(s_2(\eta)) &= \begin{cases} 0.46, & |s_2(\eta)| \leqslant 0.9, \\ 0.25, & |s_2(\eta)| > 0.9, \end{cases} & h_{26}(s_2(\eta)) &= \begin{cases} 0.43, & |s_2(\eta)| \leqslant 0.9, \\ -0.49, & |s_2(\eta)| > 0.9, \end{cases} \\ h_{31}(s_3(\eta)) &= \begin{cases} 0.49, & |s_3(\eta)| \leqslant 0.9, \\ 0.31, & |s_3(\eta)| > 0.9, \end{cases} & h_{32}(s_3(\eta)) &= \begin{cases} 0.24, & |s_3(\eta)| \leqslant 0.9, \\ -0.47, & |s_3(\eta)| > 0.9, \end{cases} \\ h_{33}(s_3(\eta)) &= \begin{cases} 0.26, & |s_3(\eta)| \leqslant 0.9, \\ -0.45, & |s_3(\eta)| > 0.9, \end{cases} & h_{36}(s_3(\eta)) &= \begin{cases} 0.48, & |s_3(\eta)| \leqslant 0.9, \\ 0.54, & |s_3(\eta)| > 0.9, \end{cases} \\ h_{41}(s_4(\eta)) &= \begin{cases} 0.45, & |s_4(\eta)| \leqslant 0.9, \\ 0.29, & |s_4(\eta)| > 0.9, \end{cases} & h_{42}(s_4(\eta)) &= \begin{cases} 0.27, & |s_4(\eta)| \leqslant 0.9, \\ -0.48, & |s_4(\eta)| > 0.9, \end{cases} \\ h_{43}(s_4(\eta)) &= \begin{cases} 0.23, & |s_4(\eta)| \leqslant 0.9, \\ -0.48, & |s_4(\eta)| > 0.9, \end{cases} & h_{46}(s_4(\eta)) &= \begin{cases} 0.42, & |s_4(\eta)| \leqslant 0.9, \\ 0.30, & |s_4(\eta)| > 0.9, \end{cases} \\ 0.52, & |s_4(\eta)| > 0.9, \end{cases} \end{cases} \end{cases}$$

$$h_{51}(s_5(\eta)) = \begin{cases} 0.53, & |s_5(\eta)| \le 0.9, \\ 0.39, & |s_5(\eta)| > 0.9, \end{cases} \quad h_{52}(s_5(\eta)) = \begin{cases} 0.28, & |s_5(\eta)| \le 0.9, \\ -0.47, & |s_5(\eta)| > 0.9, \end{cases}$$

$$h_{53}(s_5(\eta)) = \begin{cases} -0.39, & |s_5(\eta)| \le 0.9, \\ 0.52, & |s_5(\eta)| > 0.9, \end{cases} \quad h_{54}(s_5(\eta)) = \begin{cases} 0.48, & |s_5(\eta)| \le 0.9, \\ 0.39, & |s_5(\eta)| > 0.9, \end{cases}$$

$$h_{55}(s_5(\eta)) = \begin{cases} 0.27, & |s_5(\eta)| \le 0.9, \\ -0.52, & |s_5(\eta)| > 0.9, \end{cases} \quad h_{56}(s_5(\eta)) = \begin{cases} -0.36, & |s_5(\eta)| \le 0.9, \\ 0.53, & |s_5(\eta)| > 0.9, \end{cases}$$

$$h_{61}(s_6(\eta)) = \begin{cases} 0.48, & |s_6(\eta)| \le 0.9, \\ 0.28, & |s_6(\eta)| > 0.9, \\ 0.28, & |s_6(\eta)| > 0.9, \end{cases} \quad h_{62}(s_6(\eta)) = \begin{cases} 0.50, & |s_6(\eta)| \le 0.9, \\ -0.50, & |s_6(\eta)| > 0.9, \end{cases}$$

$$h_{63}(s_6(\eta)) = \begin{cases} 0.35, & |s_6(\eta)| \le 0.9, \\ 0.49, & |s_6(\eta)| > 0.9, \end{cases} \quad h_{64}(s_6(\eta)) = \begin{cases} 0.50, & |s_6(\eta)| \le 0.9, \\ 0.36, & |s_6(\eta)| > 0.9, \end{cases}$$

$$h_{65}(s_6(\eta)) = \begin{cases} 0.35, & |s_6(\eta)| \le 0.9, \\ -0.56, & |s_6(\eta)| > 0.9, \end{cases}$$

$$h_{66}(s_6(\eta)) = \begin{cases} -0.37, & |s_6(\eta)| \le 0.9, \\ 0.54, & |s_6(\eta)| > 0.9, \end{cases}$$

 $h_{ql}(y_q(\eta))$  is assigned the same value as  $h_{ql}(s_q(\eta))$ . It is not hard to obtain

$$\bar{H} = \left( \begin{array}{ccccccc} 0.72 & 0.16 & 0.66 & 0.72 & 0.17 & 0.65 \\ 0.13 & 0.18 & 0.94 & 0.17 & 0.21 & 0.92 \\ 0.18 & 0.71 & 0.77 & 0.15 & 0.71 & 0.88 \\ 0.16 & 0.75 & 0.78 & 0.12 & 0.71 & 0.89 \\ 0.14 & 0.75 & 0.91 & 0.09 & 0.79 & 0.89 \\ 0.20 & 0.81 & 0.90 & 0.14 & 0.91 & 0.91 \end{array} \right).$$

Clearly,  $g_i(\cdot)$  satisfies Assumption 2 with  $u_i = \sigma_i = 0.4$ . The parameters in the fault-tolerant controller (8) are set as  $\zeta_1 = 0.3$ ,  $\zeta_2 = 1.2$ . Select  $\Upsilon = \text{diag}(0.5013, 0.4125, 0.6324, 0.8547, 0.9063, 0.7182)$ , the matrices P and

O can be computed by using MATLAB

$$P = \begin{pmatrix} 0.4856 & 0 & 0 & 0 & 0 & 0 \\ 0 & 0.4764 & 0 & 0 & 0 & 0 \\ 0 & 0 & 0.4416 & 0 & 0 & 0 \\ 0 & 0 & 0 & 0.4583 & 0 & 0 \\ 0 & 0 & 0 & 0 & 0.4349 & 0 \\ 0 & 0 & 0 & 0 & 0 & 0.4710 \end{pmatrix}$$

$$O = \begin{pmatrix} 0.4556 & 0 & 0 & 0 & 0 & 0 \\ 0 & 0.3141 & 0 & 0 & 0 & 0 \\ 0 & 0 & 0.3609 & 0 & 0 & 0 \\ 0 & 0 & 0 & 0.3590 & 0 & 0 \\ 0 & 0 & 0 & 0 & 0.4698 & 0 \\ 0 & 0 & 0 & 0 & 0 & 0.3101 \end{pmatrix}$$

which satisfies conditions (9) and (10). By Theorem 1, through the appropriate selection of parameters for the bilayer fault-tolerant controller (8), various types of synchronization are realized.

Case 1: Take  $\delta_q^{(1)} = \frac{1}{q+3}$ , q = 1, 2, ..., 6, we can obtain  $\delta^{(1)} = \min\{\delta_q^{(1)}, q = 1, 2, ..., 6\} = 1/9$ , failure time  $\check{\eta}_{q\iota} = \hat{\eta}_{q\rho} = 0.3s$ , q = 1, 2, ..., 6,  $\iota = 4, 5, 6$ ,  $\rho = 1, 2, 3$ . Figures 1 and 2 illustrate the simulation results of the global exponential synchronization errors of networks (19) and (20) under the bilayer fault-tolerant controller (8). It is clearly observed that  $z_q(\eta)$  and  $\hat{z}_q(\eta)$  converge to zero at approximately 0.377s and 3.587s, respectively, confirming the effectiveness of the global exponential synchronization process.

Case 2: By setting  $\delta_q^{(1)} = \frac{3}{q+3}$ , q = 1, 2, ..., 6, we get  $\delta^{(1)} = \min\{\delta_q^{(1)}, q = 1, 2, ..., 6\} = 1/3$ , failure time  $\check{\eta}_{q\iota} = \hat{\eta}_{q\rho} = 0.5s$ , q = 1, 2, ..., 6,  $\iota = 4, 5, 6$ ,

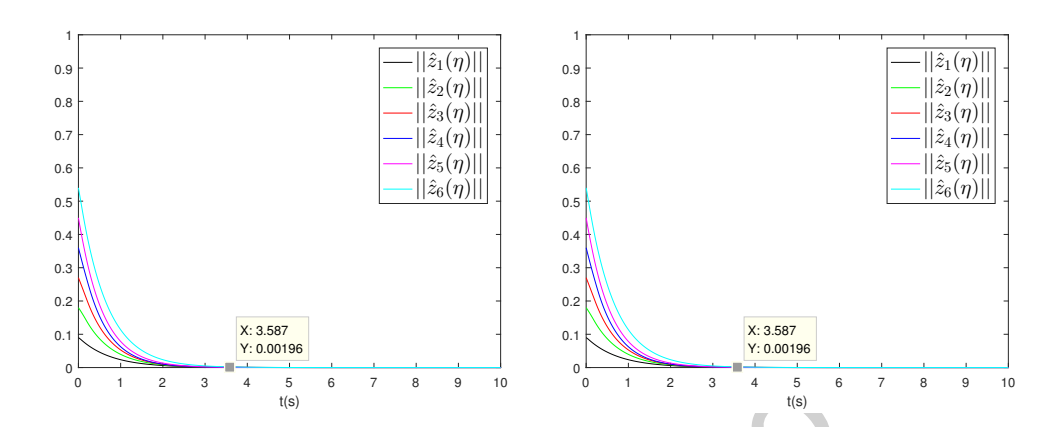


Figure 1: The norms of global exponential synchronization errors  $z_q(\eta) = y_q(\eta)$  – tial synchronization errors  $\hat{z}_q(\eta) = Q_q(\eta)$  –  $s_q(\eta), q = 1, 2, \dots, 6$ .  $M_q(\eta), q = 1, 2, \dots, 6$ .

ho=1,2,3. The values  $T(\bar{z}(0))=\frac{J^{\frac{1-\zeta_1}{2}}(\bar{z}(0))}{\delta^{(1)}(1-\zeta_1)}$  is computed as  $T(\bar{z}(0))=3.8s$ . Figures 3 and 4 present the simulation results of finite-time synchronization errors of networks (19) and (20) under the bilayer fault-tolerant controller (8) with  $T(\bar{z}(0))=3.8s$ . It is clearly observed that  $z_q(\eta)$  and  $\hat{z}_q(\eta)$  converge to zero at approximately 0.327s and 0.579s, respectively, demonstrating the effectiveness of the finite-time synchronization process.

Case 3: Set  $\delta_q^{(1)} = \frac{6}{q}$ ,  $\delta_q^{(2)} = \frac{12}{q}$ , q = 1, 2, ..., 6, we get  $\delta^{(1)} = \min\{\delta_q^{(1)}, q = 1, 2, ..., 6\} = 1$ ,  $\delta^{(2)} = \min\{\delta_q^{(1)}, q = 1, 2, ..., 6\} = 2$ , failure time  $\check{\eta}_{q\iota} = \hat{\eta}_{q\rho} = 0.4s$ , q = 1, 2, ..., 6,  $\iota = 4, 5, 6$ ,  $\rho = 1, 2, 3$ . The values  $T_{\max} = \frac{1}{\delta^{(1)}(1-\zeta_1)} + \frac{1}{(2n)^{\frac{1-\zeta_2}{2}}\delta^{(2)}(\zeta_2-1)}$  is calculated as  $T_{\max} = 4.6s$ . Figures 5 and 6 depict the simulation results of fixed-time synchronization errors of networks (19) and (20) under the bilayer fault-tolerant controller (8) with  $T_{\max} = 4.6s$ . As observed from these two figures,  $z_q(\eta)$  and  $\hat{z}_q(\eta)$  converge to zero at approximately 0.135s and 0.127s, respectively, demonstrating the effectiveness

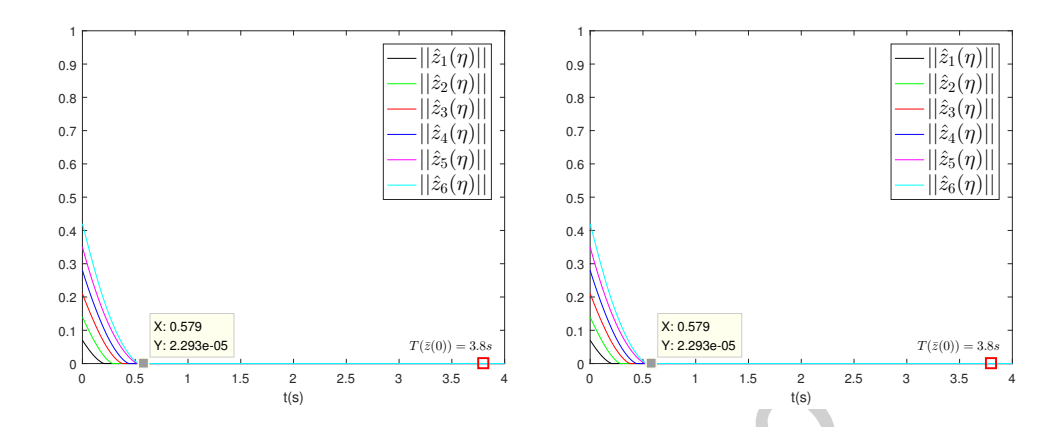


Figure 3: The norms of finite-time syn-figure 4: The norms of finite-time syn-chronization errors  $z_q(\eta) = y_q(\eta) - s_q(\eta)$ , chronization errors  $\hat{z}_q(\eta) = Q_q(\eta) - M_q(\eta)$ ,  $q = 1, 2, \dots, 6$ .

of the fixed-time synchronization process.

Case 4: Take  $T_{\delta} = 0.2s$ , failure time  $\check{\eta}_{q\iota} = \hat{\eta}_{q\rho} = 0.2s$ , q = 1, 2, ..., 6,  $\iota = 4, 5, 6$ ,  $\rho = 1, 2, 3$ . By using MATLAB,  $\delta_1^{(1)}$  and  $\delta_1^{(2)}$  can be calculated as  $\delta_1^{(1)} = \frac{\pi n^{\frac{\zeta_1}{2}}}{2^{\frac{2-\zeta_1}{2}}\zeta_1T_{\delta}} = 38.0054$ ,  $\delta_1^{(2)} = \frac{\pi}{2\zeta_1T_{\delta}} = 26.1799$ . Figures 7 and 8 depict the simulation results that show the evolution of the predefined-time synchronization errors of networks (19) and (20) under the bilayer fault-tolerant controller (8) with  $T(\delta) = 0.2s$ . It is evident that,  $z_q(\eta)$  and  $\hat{z}_q(\eta)$  converge to zero at approximately 0.048s and 0.055s, respectively, validating the efficacy of the predefined-time synchronization procedure.

From the trajectories of the control inputs, the following conclusions can be arrived at. 1) The synchronization of the drive-response MCNNs can still be ensured when effectiveness failures occur to the actuators  $k_{q\iota}$  and  $w_{q\iota}(q=1,2,\ldots,6,\iota=4,5,6)$  and bias failures occur to the actuators  $k_{q\rho}$  and  $w_{q\rho}(q=1,2,\ldots,6,\rho=1,2,3)$ . 2) Even if actuator failure occurs at

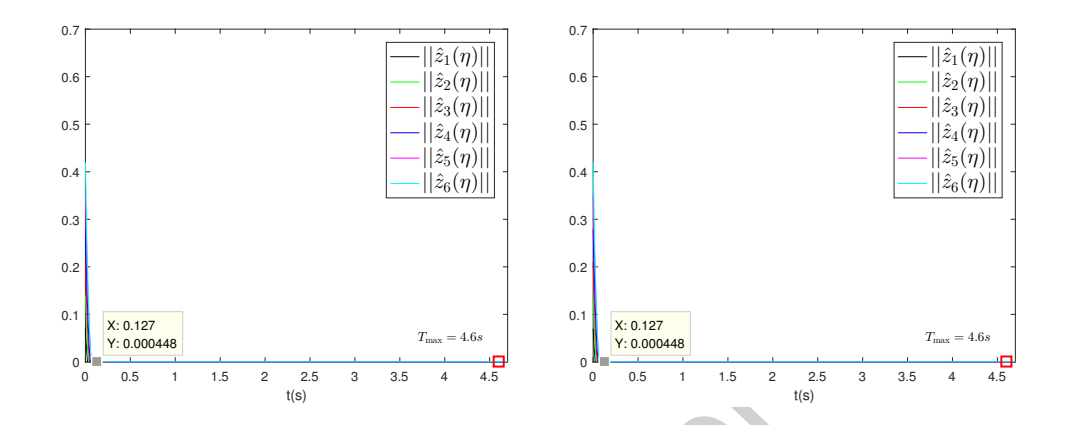


Figure 5: The norms of fixed-time syn-figure 6: The norms of fixed-time syn-chronization errors  $z_q(\eta) = y_q(\eta) - s_q(\eta)$ , chronization errors  $\hat{z}_q(\eta) = Q_q(\eta) - M_q(\eta)$ ,  $q = 1, 2, \dots, 6$ .

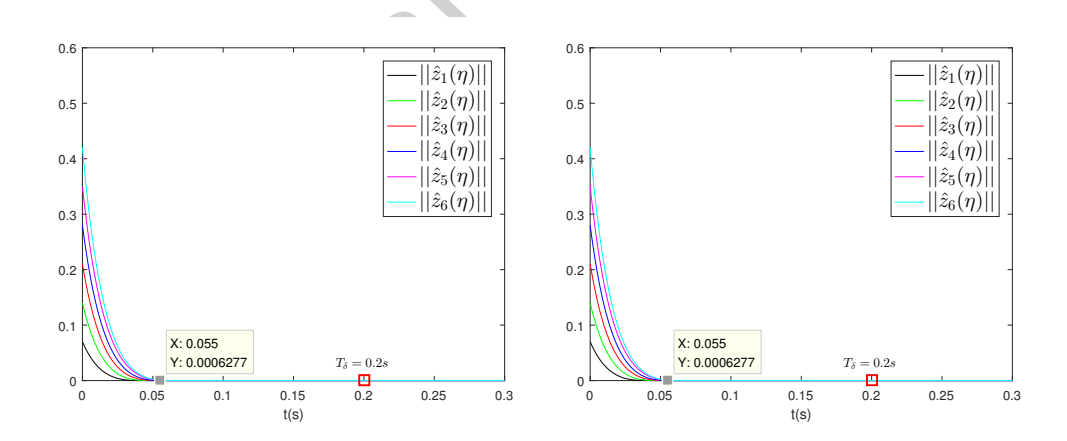


Figure 7: The norms of predefined-time Figure 8: The norms of predefined-time synchronization errors  $z_q(\eta) = y_q(\eta)$  – synchronization errors  $\hat{z}_q(\eta) = Q_q(\eta)$  –  $s_q(\eta), q = 1, 2, \dots, 6$ .

different time point, bilayer fault-tolerant controller (8) can still guarantee the synchronization of the simulation system. 3) Under the bilayer fault-tolerant controller (8), the synchronization performance within the predefined time of the drive-response MCNNs is the best. These results collectively indicate that the bilayer fault-tolerant controller (8) developed in this study is reliable.

Remark 7. In practical control systems, actuators may suffer from both effectiveness and bias failures, and these two types of failure can even occur simultaneously. However, most existing studies only takes effectiveness failures into account [41, 42], while neglecting the combined impact of the two failure modes on system performance and stability. To tackle this limitation, we propose a bilayer fault-tolerant control scheme for drive-response MCNNs, which is capable of handling both types of faults. The layered structure not only enhances the clarity of controller design and stability analysis, but also boosts the flexibility of parameter tuning. Furthermore, MCNNs incorporate competition characteristics, which endow them with greater expressiveness and make them more suitable for complex tasks compared to traditional MNNs. The simulation results presented in this section confirm that our proposed method successfully achieves four types of synchronization – exponential, finite-time, fixed-time, and predefined-time – under the coexistence of bias and effectiveness faults. These results not only validate the theoretical analysis but also demonstrate the robustness of the proposed fault-tolerant control scheme in static fault scenarios. That is to say, the current work does not take varying failure patterns into account, such as time-varying or aperiodically intermittent actuator faults. However, in real-world applications,

faults may occur intermittently or evolve over time, which poses additional challenges to controller design. Some recent studies have explored such fault patterns by adopting time-varying [53, 54] and intermittent [55, 56] fault-tolerant control strategies. Nevertheless, incorporating these complex failure modes into the MCNN framework remains an open and meaningful research problem. In the near future, it would be valuable to extend our results to handle time-varying delay or intermittent actuator failures, which would further enhance the practicality and reliability of the proposed control scheme.

#### 5. Conclusions

This paper centers around addressing four types of fault-tolerant synchronization issue regarding drive-response MCNNs in the event of multiple actuator failures. The failures under study involve both bias and effective-ness failures. By employing a suitable Lyapunov functional along with inequality techniques, the bilayer fault-tolerant controller has been properly designed. Through the adjustment of controller parameters, the global exponential synchronization, finite-time synchronization, fixed-time synchronization, and predefined-time synchronization of the drive-response MCNNs can be respectively achieved. Finally, simulation examples with detailed analysis and comparison are provided to verify the feasibility of the obtained results. In the future, it would be very interesting to further explore the synchronization problem of MCNNs with multiple actuator failures by using some advanced fault-tolerant control approaches. More specifically, possible directions include improving robustness against external disturbances and parameter uncertainties, addressing time-varying delays, and develop-

ing adaptive strategies to estimate fault parameters. Additionally, extending the proposed approach to more complex network structures, such as coupled MCNNs, would further enhance their practical value.

### Acknowledgments

The authors would like to thank the Editor and anonymous reviewers for their valuable comments and suggestions for improving this manuscript. This work was supported by the National Natural Science Foundation of China under Grant 62173244.

#### References

#### References

- [1] H. Wang, Y. Zou, X. J. Liu, Z. Y. Meng, A rapid time synchronization scheme using virtual links and maximum consensus for wireless sensor networks, IEEE Internet of Things Journal, 12 (3) (2025) 3318-3329.
- [2] G. Marti, F. Arquint, C. Studer, Jammer-resilient time synchronization in the MIMO uplink, IEEE Transactions on Signal Processing, 73 (2025) 706-720.
- [3] C. L. Da, F. Li, L. F. Wang, C. X. Tao, S. F. Li, M. Nie, Pulse synchronization scheme for undersea BWPT system based on simultaneous wireless power and data transfer technology, IEEE Transactions on Circuits and Systems II: Express Briefs, 72 (1) (2025) 333-337.

- [4] X. N. Song, X. L. Sun, S. Song, S. Y. Xu, A novel event-triggered bipartite consensus for PDE-based multiagent systems with switching topologies and antagonistic interactions, IEEE Transactions on Cybernetics, 54 (10) (2024) 5759-5769.
- [5] W. T. Wang, J. H. Wu, W. Chen, The characteristics method to study global exponential stability of delayed inertial neural networks, Mathematics and Computers in Simulation, 232 (2025) 91-101.
- [6] E. Y. Cong, L. Zhu, X. Zhang, Global exponential synchronization of discrete-time high-order BAM neural networks with multiple timevarying delays, AIMS Mathematics, 9 (12) (2024) 33632-33648.
- [7] Y. Chen, S. Zhu, H. C. Yan, M. Q. Shen, X. Y. Liu, S. P. Wen, Event-based global exponential synchronization for quaternion-valued fuzzy memristor neural networks with time-varying delays, IEEE Transactions on Fuzzy Systems, 32 (3) (2024) 989-999.
- [8] G. Kamenkov, On stability of motion over a finite interval of time, Journal of Applied Mathematics and Mechanics, 17 (2) (1953) 529-540.
- [9] X. H. Liu, Y. F. Li, G. J. Xu, Finite-time synchronization analysis for the generalized caputo fractional spatio-temporal neural networks, Mathematics and Computers in Simulation, 230 (2025) 94-110.
- [10] L. X. Lin, Finite-time synchronization of memristor-based neural networks: energy cost estimation, International Journal of Dynamics and Control, 11 (2) (2023) 738-747.

- [11] A. J. Wang, Z. L. Yang, X. Wang, J. Zhang, M. J. Li, Finite-time synchronization of delayed complex network under event-dependent intermittent control, Control and Decision, 39 (11) (2024) 3673-3680.
- [12] A. A. Wei, Z. Y. Yao, Y. Zhang, K. M. Wang, Finite-time synchronization of delayed semi-markov reaction-diffusion systems: an asynchronous boundary control scheme, ISA Transactions, 148 (2024) 326-335.
- [13] A. Abdurahman, R. Tohti, C. C. Li, New results on fixed-time synchronization of impulsive neural networks via optimized fixed-time stability, Journal of Applied Mathematics and Computing, 70 (4) (2024) 2809-2826.
- [14] Z. J. Liu, Y. F. Pu, X. Y. Hua, X. X. You, Robust fixed-time synchronization of fuzzy shunting-inhibitory cellular neural networks with feedback and adaptive control, International Journal of Adaptive Control and Signal Processing, 38 (7) (2024) 2320-2339.
- [15] J. Liu, Y. B. Wu, C. X. Mu, C. Y. Sun, Aperiodically intermittent fixedtime synchronization of coupled reaction-diffusion systems via average control rate, IEEE Transactions on Systems, Man, and Cybernetics: Systems, 55 (2) (2025) 963-975.
- [16] J. Y. Ran, T. C. Zhang, Fixed-time synchronization control of fuzzy inertial neural networks with mismatched parameters and structures, AIMS Mathematics, 9 (11) (2024) 31721-31739.
- [17] M. J. Zhang, H. Y. Zang, Z. D. Shi, A unified Lyapunov-like char-

- acterization for predefined time synchronization of nonlinear systems, Nonlinear Dynamics, 112 (11) (2024) 8775-8787.
- [18] T. B. Lopez-Garcia, J. A. Domínguez-Navarro, Optimal power flow with physics-informed typed graph neural networks, IEEE Transactions on Power Systems, 40 (1) (2025) 381-393.
- [19] S. Batreddy, P. Mishra, Y. Kakarla, A. Siripuram, Inpainting-driven graph learning via explainable neural networks, IEEE Signal Processing Letters, 32 (2025) 111-115.
- [20] S. X. Lai, W. N. Luan, J. Tao, Explore your network in minutes: a rapid prototyping toolkit for understanding neural networks with visual analytics, IEEE Transactions on Visualization and Computer Graphics, 30 (1) (2024) 683-693.
- [21] M. A. Cohen, S. Grossberg, Absolute stability of global pattern formation and parallel memory storage by competitive neural networks, IEEE Transactions on Systems, Man, and Cybernetics, 13 (5) (1983) 815-826.
- [22] Y. L. Yang, Y. T. Liu, Global exponential convergence and synchronization for exponential numerical competitive neural networks with different time scales and fuzzy logic, Proceedings of the Institution of Mechanical Engineers, Part C: Journal of Mechanical Engineering Science, 238 (14) (2024) 6795-6812.
- [23] A. R. Subhashri, T. Radhika, Robust dissipativity analysis for stochastic markov jump competitive neural networks with mixed delays, Journal of Applied Mathematics and Computing, 71 (1) (2025) 801-828.

- [24] X. B. Nie, B. Q. Cao, W. X. Zheng, J. D. Cao, Multistability analysis of fractional-order state-dependent switched competitive neural networks with sigmoidal activation functions, IEEE Transactions on Systems, Man, and Cybernetics: Systems, 55 (3) (2025) 2106-2119.
- [25] S. T. Chen, Y. Wan, J. D. Cao, J. Kurths, Predefined-time synchronization for competitive neural networks with different time scales and external disturbances, Mathematics and Computers in Simulation, 222 (2024) 330-349.
- [26] D. B. Strukov, G. S. Snider, D. R. Stewart, R. S. Williams, The missing memristor found, Nature, 453 (2008) 80-83.
- [27] Q. M. Wang, L. M. Wang, W. D. Wen, Y. Li, G. D. Zhang, Dynamical analysis and preassigned-time intermittent control of memristive chaotic system via T-S fuzzy method, Chaos, 35 (2025) 023102.
- [28] L. M. Wang, Q. M. Wang, G. D. Zhang, Adaptive intermittent stabilization of memristive chaotic system via TS fuzzy model, IEEE Transactions on Circuits and Systems II: Express Briefs, 71 (3) (2024) 1351-1355.
- [29] X. N. Song, J. T. Man, J. H. Park, S. Song, Finite-time synchronization of reaction-diffusion inertial memristive neural networks via gain-scheduled pinning control, IEEE Transactions on Neural Networks and Learning Systems, 33 (9) (2022) 5045-5056.
- [30] X. N. Song, J. T. Man, S. Song, C. K. Ahn, Gain-scheduled finitetime synchronization for reaction-diffusion memristive neural networks

- subject to inconsistent Markov chains, IEEE Transactions on Neural Networks and Learning Systems, 32 (7) (2021) 2952-2964.
- [31] C. G. Xu, M. H. Jiang, J. H. Hu, Fixed-time synchronization of complexvalued memristive competitive neural networks based on two novel fixedtime stability theorems, Neural Computing and Applications, 35 (30) (2023) 22605-22620.
- [32] S. S. Ren, Y. Zhao, Y. H. Xia, Anti-synchronization of a class of fuzzy memristive competitive neural networks with different time, Neural Processing Letters, 52 (1) (2020) 647-661.
- [33] M. Sader, F. Y. Wang, Z. X. Liu, Z. Q. Chen, General decay projective synchronization of memristive competitive neural networks via nonlinear controller, International Journal of Nonlinear Sciences and Numerical Simulation, 23 (6) (2022) 867-878.
- [34] S. Q. Gong, S. F. Yang, Z. Y. Guo, T. W. Huang, Global exponential synchronization of memristive competitive neural networks with timevarying delay via nonlinear control, Neural Processing Letters, 49 (1) (2019) 103-119.
- [35] X. N. Song, M. Wang, C. K. Ahn, S. Song, Finite-time fuzzy bounded control for semilinear PDE systems with quantized measurements and Markov jump actuator failures, IEEE Transactions on Cybernetics, 52 (7) (2022) 5732-5743.
- [36] S. Song, J. H. Park, B. Y. Zhang, X. N. Song, Adaptive NN finite-time resilient control for nonlinear time-delay systems with unknown

- false data injection and actuator faults, IEEE Transactions on Neural Networks and Learning Systems, 33 (10) (2022) 5416-5428.
- [37] Z. J. Zhao, Y. Ren, C. X. Mu, T. Zou, K. S. Hong, Adaptive neural-network-based fault-tolerant control for a flexible string with composite disturbance observer and input constraints, IEEE Transactions on Cybernetics, 52 (12) (2022) 12843-12853.
- [38] Z. J. Zhao, Z. J. Liu, W. He, K. S. Hong, H. X. Li, Boundary adaptive fault-tolerant control for a flexible Timoshenko arm with backlash-like hysteresis, Automatica, 130 (2021) 109690.
- [39] X. S. Yang, X. D. Li, J. Q. Lu, Z. S. Cheng, Synchronization of timedelayed complex networks with switching topology via hybrid actuator fault and impulsive effects control, IEEE Transactions on Cybernetics, 50 (9) (2020) 4043-4052.
- [40] P. Selvaraj, R. Sakthivel, C. K. Ahn, Observer-based synchronization of complex dynamical networks under actuator saturation and probabilistic faults, IEEE Transactions on Systems, Man, and Cybernetics: Systems, 49 (7) (2019) 1516-1526.
- [41] J. P. Zhou, Y. M. Liu, J. W. Xia, Z. Wang, S. Arik, Resilient fault-tolerant anti-synchronization for stochastic delayed reaction-"diffusion neural networks with semi-Markov jump parameters, Neural Networks, 125 (2020) 194-204.
- [42] X. S. Yang, X. X. Wan, Z. S. Cheng, J. D. Cao, L. Yang, L. Rutkowski, Synchronization of switched discrete-time neural networks via quantized

- output control with actuator fault, IEEE Transactions on Neural Networks and Learning Systems, 32 (9) (2021) 4191-4201.
- [43] M. X. Wang, S. L. Zhu, S. M. Liu, Y. Du, Y. Q. Han, Design of adaptive finite-time fault-tolerant controller for stochastic nonlinear systems with multiple faults, IEEE Transactions on Automation Science and Engineering, 20 (4) (2023) 2495-2502.
- [44] Z. Guo, S. Yang, J. Wang, Global exponential synchronization of multiple memristive neural networks with time delay via nonlinear coupling, IEEE Transactions on Neural Networks and Learning Systems, 26 (6) (2015) 1300-1311.
- [45] Y. Chen, S. Zhu, M. Shen, X, Liu, S. Wen, Event-based output quantized synchronization control for multiple delayed neural networks, IEEE Transactions on Neural Networks and Learning Systems, 35 (1) (2024) 428-438.
- [46] S. P. Bhat, D. S. Bernstein, Finite-time stability of continuous autonomous systems, SIAM Journal on Control and Optimization, 38 (3) (2000) 751-766.
- [47] A. Polyakov, Nonlinear feedback design for fixed-time stabilization of linear control systems, IEEE Transactions on Automatic Control, 57 (8) (2012) 2106-2110.
- [48] J. D. Sánchez-Torres, D. Gómez-Gutiérrez, E. López, A. G. Loukianov, A class of predefined-time stable dynamical systems, IMA Journal of Mathematical Control and Information, 35 (1) (2018) 1-29.

- [49] A. Wu, Y. Chen, Z. Zeng, Multi-mode function synchronization of memristive neural networks with mixed delays and parameters mismatch via event-triggered control, Information Sciences, 572 (2021) 147-166.
- [50] M. X. Wang, S. Zhu, M. Q. Shen, X. Y. Liu, S. P. Wen, Fault-tolerant synchronization for memristive neural networks with multiple actuator failures, IEEE Transactions on Cybernetics, 54 (9) (2024) 5092-5101.
- [51] C. A. Anguiano-Gijón, A. J. Muñoz-Vázquez, J. D. Sánchez-Torres, G. Romero-Galván, F. Martínez-Reyes, On predefined-time synchronisation of chaotic systems, Chaos Solitons and Fractals, 122 (2019) 172-178.
- [52] G. H. Hardy, J. E. Littlewood, G. Pólya, Inequalities, Cambridge University Press, 1952.
- [53] D. Z. Zhao, L. L. Cui, D. D. Lui, Adaptive demodulation synchroextracting transform for bearing time-varying fault feature extraction, Proceedings of the Institution of Mechanical Engineers Part C-Journal of Mechanical Engineering Science, 238 (13) (2024) 6103-6116.
- [54] X. F. Zhao, X. W. Li, J. Z. Zhang, Z. Zhang, Active fault-tolerant control scheme for unmanned air-ground attitude system with time-varying delay faults, Applied Sciences, 12 (12) (2022) 5882.
- [55] L. L. Yang, S. M. Zhou, W. X. Zheng, Hybrid intermittent fault diagnosis of general graphs, Discrete Applied Mathematics, 374 (2025) 16-32.
- [56] X. P. Fang, H. J. Fan, L. Liu, W. Wang, B. Wang, Adaptive event-triggered control for uncertain nonlinear systems with multiple inter-

mittent actuator faults of uncertain directions, ISA Transactions, 161 (2025) 14-23.



### **Declaration of interests**

☑ The authors declare that they have no known competing financial interests or personal relationships that could have appeared to influence the work reported in this paper.
☐ The authors declare the following financial interests/personal relationships which may be considered as potential competing interests:

#### Authors' Biographies

#### I. Biography of Yanli Huang:



Yanli Huang received her Ph.D. degree in applied mathematics from School of Mathematics and System Sciences, Beihang University, China, in 2012.

Currently, she is a professor in the School of Computer Science and Technology, Tiangong University. Her research interests include complex dynamical networks, synchronization, passivity and stability theory.

#### II. Biography of Wenjing Duan:



Wenjing Duan received her B.S. degree in computer science and technology from School of Intelligent Engineering, Zhengzhou University of Aeronautics, China, in 2023.

She is currently a graduate student at School of Computer Science and Technology, Tiangong University. Her research interests include neural networks and predefined-time synchronization.

#### III. Biography of Quang Dan Le:



Quang Dan Le received his Ph.D. degree from School of Electrical Engineering, University of Ulsan, South Korea, in 2022.

Currently, he is a lecturer in the College of Science and Engineering, University of Derby. His research interests include teleoperation, wearable haptics, robotics inspire and fault-tolerant control.

#### IV. Biography of Tse Chiu Wong:



**Tse Chiu Wong** received his Ph.D. degree in Operations Research from the University of Hong Kong, China, in 2008.

Currently, he is a senior lecturer in the department of Design Manufacturing and Engineering Management, University of Strathclyde. His research interests include

operations research, neural computing and soft computing.

